Universitetet
i Stavanger

FACULTY OF SCIENCE AND TECHNOLOGY

MASTER'S THESIS

STUDY PROGRAM/ SPECIALIZATION:	SPRING SEMESTER, 2017
Biological Chemistry/Cancer Metabolism	RESTRICTED ACCESS
WRITER: Abdelnour Alhourani	(WRITER'S SIGNATURE)
FACULTY SUPERVISOR: Associate Professor Hanne Røland Hagland	

THESIS TITLE:

METABOLIC ASSESSMENT OF METFORMIN TREATMENT IN COLON CANCER CELLS

CREDITS (ECTS): 60

KEY WORDS:	PAGES: 73 +ENCLOSURE: 80
Colorectal Cancer, Metformin, Targeting mitochondria, Glycolytic cancer cell-line	STAVANGER, 31,05,17

ABSTRACT

Resistance against traditional chemotherapy is a challenge in the treatment of colorectal cancer (CRC). The use of metformin, a commonly prescribed biguanide anti-diabetic drug, has shown to correlate with cancer preventive and antineoplastic effects in CRC. By targeting the mitochondria of cancer cells, metformin may be able to prevent cancer relapse caused by cells resistant to standard chemotherapy termed stem-like cancer cells (CSCs). The aim of this project was therefore to assess the growth inhibitory effects and metabolic changes in a colon cancer cell model with a glycolytic phenotype. The results indicate that metformin was able to moderately affect the metabolic homeostasis and cause a slight growth reduction in these cell lines, which was most prominent when grown in cell medium containing physiological levels of glucose. These effects were seen using metformin dosage within the therapeutic approved range and indicate that metformin could be an interesting adjuvant drug to be utilized in CRC treatment.

ACKNOWLEDGMENTS

I would like to express my gratitude to the wonderful people who have been instrumental in accomplishing this work. First and foremost, I would like to thank my thesis supervisor Associate Professor Hanne Røland Hagland for her constant academic and moral support. She devoted an immense amount of time to thoroughly explain the conceptional, analytical and technical aspects of this work which significantly increased my interest and passion for this research and scientific inquiry in general. I am grateful to have been part of her research group and under her mentorship, not only due to her high dedication for helping everyone in the group but also for her receptive and encouragement towards original thinking. I would also like to thank the advisor at UiS international office Magdalena Brekke for her kind help and support since day one of my scholarship and for her genuine concerns.

I would like to acknowledge and thank all the academic staff at the Centre for Organelle Research (CORE), mainly the lab members who graciously helped in sharpening my technical skills, especially Julie Nikolaisen for her outstanding assistance in different aspects of this thesis. I would also like to thank the professors who taught me throughout my master's. Namely, Professor Lutz Eichacker for all the insightful conversations and critical advises. Also, Professor Peter Ruoff for greeting everyone into the faculty and introducing me to my current supervisor.

Last but not least, I would like to thank my friends, close and distant. My father for his endless support and encouragement towards gaining more knowledge, even when the circumstances were not ideal. My mother and sister for standing by my side through thick and thin and offering unconditional love and support.

CONTRIBUTIONS

With the guidance of my supervisor, Associate Professor Hanne Røland Hagland, I have designed and completed the experiments and analysed the results. Thanks to our collaborators, the "Gastrointestinal translational research unit" at Stavanger University Hospital for supplying the cell-line.

I would like to specifically recognise the contributions of the following lab members and research associates for their advices carrying out various experiments. Johannes Lange for his help in the cell-lab. Kristin Aaser Lunde, Maria Creighton, Stefanie Lackner, Dugassa Nemie-Feyissa for their inputs towards accomplishing western blot tasks. Jodi Grødem, Marthe Gurine Førland, Xiang Ming Xu for their training and help performing confocal imaging. Also, Marina Alexeeva and René Pedersen for their help in various scenarios and my lab partner Ansooya Bokil for her assistance throughout long working hours. Finally, I would like to express my deepest gratitude towards Julie Nikolaisen and Tia Tidwell for their great help in various parts of the thesis especially in training me to perform the flow cytometry and qPCR experiments.

I am grateful for CORE and the University of Stavanger for awarding me this 2-year masters scholarship in collaboration with Norwegian Centre for International Cooperation in Education (SIU) which brought me back on track in pursuing higher degrees and helped financially throughout my study period.

TABLE OF CONTENTS

LIST OF ABBREVIATIONS

CRC	:	Colorectal Cancer
CINS	:	chromosomal instability
APC	:	Adenomatous polyposis coli gene
WNT	:	Wingless-type MMTV integration site family
MMR	:	DNA mismatch repair system
MSI	:	microsatellite instability
CIMP	:	CpG island methylator phenotype
MGMT	:	O-6-methylguanine-DNA methyltransferase
MLH1	:	MutL homolog 1
SFRPS	:	Secreted frizzled-related protein 1
TCA	:	Tricarboxylic acid-cycle
SAM	:	S-adenosylmethionine
SAH	:	S-Adenosyl-L-homocysteine
ATP	:	adenosine triphosphate
NAD	:	Nicotinamide adenine dinucleotide
LSD1	:	Lysine-specific demethylase 1
TET	:	Ten-eleven translocation methylcytosine dioxygenase
FAD	:	Flavin adenine dinucleotide
T2D	:	Type 2 Diabetes
DHA	:	Docosahexaenoic acid
HDAC1	:	Histone deacetylase 1
HIF	:	Hypoxia-inducible factor
GLUT	:	Glucose transporter
NADPH	:	Nicotinamide adenine dinucleotide phosphate
PPP	:	Pentose phosphate pathway
AMP	:	Adenosine monophosphate
CAMKKB	:	calmodulin-dependent protein kinase kinase b
TAK1	:	TGF-b-activated kinase-1
MTORC1	:	mammalian target of rapamycin complex 1
LKB1	:	liver kinase B1
TSC2	:	tuberous sclerosis complex2
PI3K	:	Phosphoinositide 3-kinase
RTKS	:	Receptor tyrosine kinase
PIP2,3	:	Phosphatidylinositol 4,5-bisphosphate
RHEB	:	Ras homolog enriched in brain
GSK-3B	:	Glycogen synthase kinase 3 beta
AKT	:	Protein kinase B
AMPK	:	AMP-activated protein kinase

IGF1R	:	Insulin-like growth factor 1 receptor
4EBP1	:	translation initiation factor 4E-binding protein 1
P70S6K	:	S6 ribosomal protein via p70S6 kinase
S6RP	:	Phosphorylated S6 ribosomal protein
ETC	:	electron transport chain
UCP	:	uncoupling protein
HKII	:	hexokinase II
GPCRS	:	G-protein-coupled receptors
PTEN	:	Phosphatase and tensin homolog
PDK1	:	Pyruvate dehydrogenase lipoamide kinase isozyme 1
EGFR	:	epidermal growth factor receptor
KRAS	:	Kirsten rat sarcoma viral oncogene homolog
PIK3CA	:	Phosphatidylinositol 4,5-bisphosphate 3-kinase catalytic subunit alpha isoform
PIK3R1	:	Phosphatidylinositol 3-kinase regulatory subunit alpha
SGLT	:	Sodium-glucose transport proteins
FOXO	:	Forkhead box O
ROS	:	Reactive oxygen species
NSAIDS	:	Nonsteroidal anti-inflammatory drug
VEGF	:	Vascular endothelial growth factor
COX	:	Cyclooxygenase
PGE2	:	Prostaglandin E2
CSCS	:	cancer stem cells
CCCS	:	chemo-resistant cancer cells
OXPHOS	:	Oxidative phosphorylation
OCTS	:	Organic cation transport proteins
PMAT	:	plasma membrane monoamine transporter
IGF-1	:	Insulin-like growth factor 1
IR-A	:	Insulin receptor isoform A
ATM	:	ataxia telangiectasia mutated
HER2	:	Human Epidermal Growth Factor Receptor 2
MGPD	:	mitochondrial glycerol-phosphate dehydrogenase
FAS	:	Fatty acid synthase
ACC	:	Acetyl-CoA carboxylase
SREBP-1	:	Sterol regulatory element-binding protein 1
SIRT1	:	Sirtuin 1
5-FU	:	5-Fluorouracil
RORA	:	RAR Related Orphan Receptor A

LIST OF TABLES

LIST OF FIGURES

CHAPTER 1. LITERATURE REVIEW

1.1 INTRODUCTION

Since its first mention by Hippocrates in 360 BCE, cancer have been and remains to be an abstruse disease to medicine throughout history. Initially described by the Greeks as a "carb-like" illness caused by an excess of black bile, the comprehension of its pathophysiology, etiology, prognosis and treatment options have progressed slowly over the years. A significant milestone in cancer treatment was not seen until the seventeenth century, when *Wilhelm Fabricus* provided an adequate operational descriptions for various cancers [1]. Since then, the increased cancer incident provoked more investigations into its underlying mechanisms, leading to today's understanding of it being a complex disease of the cell. The criteria of this cancer cell are hallmarked by a commonly agreed major attributes. Aggressiveness, through auto-growth signalling prompting a rapid proliferation. As well as unresponsiveness, manifesting in the loss of contact inhibition and apoptosis evasion. In addition to self-indulgence by promoting angiogenesis and replicating indefinitely until possibly metastasizing to other tissues [2]. Yet, modern medicine is still unable to restrain the continuously increasing cancer-related mortalities, almost doubled in numbers over the last 4 decades to become only second to cardiovascular diseases and expected to further duplify in the upcoming couple of decades [1,2,3].

Several theories were put in place to explain the increasing incidents of cancers in modern days compared to the much lower mentioned occurrence in earlier civilizations. Most commonly it has been attributed to an ageing population reaching a lifespan of 90 years compared to 5 centuries ago when the elite had a life expectancy of 45, while lower classes usually lived up to their 30s. Still, considering the historical scarcity of cancers that are known to develop in younger population, namely bone cancer gave more significance to the involvement of carcinogenic environmental factors in modern societies which is now linked up to 75% of human cancers [1]. Nonetheless, a clear, unified origin of cancers is still highly debated. The majority of current research focuses on the genetic aspects of the disease, discovering a never-ending cancer-related gene mutations and driving numerous targeted therapies to materialize. Howbeit, their outcomes on a mortality scale is not satisfying. New directions are emerging in cancer treatment, investigating the use of nontoxic metabolic therapies to manage cancers [2].

this thesis is aimed to discuss the metabolic mechanisms of cancers, mainly the ones altering mitochondrial functions due to its pivotal roles in cancer adaptations [4] and its possible targeting for cancer therapy. *In-vitro* research takes the case of colorectal cancer and the possibility of utilizing a worldwide available, relatively cheap antidiabetic drug, metformin as an adjuvant treatment. The evaluation is carried on using a metabolically profiled colorectal cancer cell line and regards the metabolic altering aspects while observing changes in suspected biomarkers.

1.2 COLORECTAL CANCER

In a world where modern medicine introduced a major transition towards non-communicable disease, colorectal cancer (CRC) is emerging as a serious burden to public health. Regarded the third most common cancer worldwide, with over 1 million new incidents each year (roughly a tenth of all cancer incidents). CRC accounts for an approximate of 600,000 annual mortalities with less than 20% 5-year survival in metastatic cases [3,5,6].

Most of CRC incidences are of a sporadic (nonhereditary) origin, diagnosed mainly in populations older than 50 years. Albeit its foreseen that every other person would develop adenomatous polyp by the age of 70, only 10% of the cases progress to CRC, elucidated by the molecular heterogeneity of these polyps, despite their homogeneous tubular histological appearance [3,6].

The initiation of dysplastic adenomatous polyps has been proposed to originate from a stem-like cell residing in the base of the colon crypts eventually leading to adenocarcinoma in over 95% of CRC incidents, this is driven by the accumulation of acquired genetic alterations resulting in molecular abnormalities which characterizes the multistep progression of sporadic CRC from normal colonic epithelium [6,7]. Evidence of environmental risk factors involvement is associated with its high prevalence in developed countries [3,6,7].

Geographical differences in CRC prevalence highlights the role of modifiable lifestyle factors in disease incident. These factors encompass the consumption of red/processed meat, smoking, alcohol and obesity. Contrarily, enhanced dietary habits like increased

fiber intake, reliance on whole grains and the consumption of milk well as physical activity is proposed to reduce the risk of these factors [3]. Admittingly, the involvement of environmental factors in CRC seems to increase the disease complexity, however, they provide a strong incentive towards investigating the underlying molecular carcinogenic events at pace with the genetic discoveries that seen a tremendous latent progress [5].

1.2.1 EPIGENETICS, MODIFIABLE RISK FACTORS AND CELLULAR METABOLISM CROSSTALK IN CRC

The subsequent variety of determinants incorporating the onset of CRC have not changed, to date, the disorder being recognized to be of genetic roots, reshaping the cell genome through three main pathways (Fig.1 A). The primary source of genomic alterations in CRC is the *chromosomal instability* (CINs) [8]. Deformities in the segregation of chromosomes, centromere and telomere dysfunctions, loss of heterozygosity and deficiencies in DNA repair mechanisms are the main grounds to develop CINs. In 85% of sporadic CRCs, CINs are responsible for chromosomal rearrangements of which abnormalities in *APC* and the Wnt Pathway are known to be the first victims (Fig.1 A1) [5,8,9].

Next in order is *microsatellite instability* (MSI). Consequential of defects in the DNA mismatch repair (MMR) system (Fig.1 A2), MSI is responsible for increasing the mutation rate in more than 15% of sporadic CRCs. In a very close relation comes the *CpG island methylator phenotype* (CIMP). As the name suggests, it is an aberrant DNA methylation epigenetically silencing promoters located in genomic areas rich in CpG dinucleotides pockets termed CpG islands and found in 20–30 % of CRC (Fig.1 A3). The last mechanism could be responsible for disturbing DNA repair through the silencing of *MGMT* and *MLH1* in addition to switching off tumour suppressors like *SFRPs* and Wnt signalling antagonists [5,8,9]. Interestingly, MSI and CIMP mutual contribution to sporadic CRC is explained through the hypermethylation of the *MLH1* gene, which encodes MutL homolog 1, a central protein to MMR mismatch recognition and repair [5,9]. This indicates the cell ability to alter its gene expression which will be explored further in later paragraphs.

Alterations to metabolism have been long observed in all cancers, one modification that seems to be characteristic to most, and now a recognised hallmark of cancer, is the increased dependency on glycolysis out of necessity to encompass extensive growth among other metabolic shifts occurring in cancer cells (Fig.1 B) [2,10].

Numerous minor metabolic changes are found to be distinct to each cancer type, and CRC is no exception, adding a layer of specificity to the metabolic activity of various cancers. A recent study in metabolomics aiming to differentiate colon from ovarian cancer revealed compelling divergence in over 60 metabolites individualising colon cancer metabolic signature [11]. While that could prove helpful in tracing back the cancers to originating tissues, therefore, differentiating primary cancers from metastasis as the previous study directs, this also underscores the underlying heterogeneous metabolic activity of distinct cancer phenotypes. Findings from the previously mentioned study demonstrate a comparative decline in TCA cycle metabolism of CRC opposed with an elevated β-oxidation and urea cycle activity [11]. Acknowledging that these metabolic variations are of a metabolic reprogramming origin, leads to the notion in which the modified cellular metabolism encompassing unique local metabolite concentrations maintains a reciprocal relationship with the modifications seen on a genomic level through epigenetic modulation [9;12].

Furthermore, some of these metabolites derived from TCA cycle and glycolysis demonstrate the capacity to obtain an oncogenic profile, regulating gene expression and cell signalling by being indispensable cofactors for chromatin-modifying pathways through different biochemical processes (Fig.1 B). The first being acetylation, occurring by virtue of the accumulated glycolysis intermediate acetyl-CoA, subsequent to the increased glucose uptake. Acetyl-CoA can donate its acetyl group to the lysine in histones promoting the acetylation of the latter and therefore modify gene expression [9,12,13]. Methylation is a clear second. In a similar fashion, the methyl containing SAM, a one-carbon metabolism cycle product, can potentially cause DNA and histone methylation. The controlling mechanism in normal situation is mandated by the fact that each time SAM loses its methyl group, it results in SAH, an inhibitor of the methylation critical enzyme, methyltransferase. However, SAM could still cause hypermethylation in a scenario where it is overproduced. Given that SAM is a product of L-methionine and ATP, such scenario is possible considering cancer's increased energy production [9,13]. Other alterations in metabolite levels originating from the energetic shift of cancer cells includes low NAD+/NADH ratios inducing histone acylation in correlation with glucose concentrations, as well as α-Ketoglutarate and LSD1 mediated DNA demethylation by TET proteins and FAD respectively (Fig.1 B) [12,13].

Aside from the interchangeable relation between metabolism and oncogenes in promoting carcinogenesis, a collective of modifiable risk factors are known to boost the

acquisition of hallmark cancer behaviours through either direct-genetic or metabolic mediated-epigenetic means. These factors, which arise from modern lifestyle and diet could be held accountable for the increased numbers of CRC occurrence in developed countries [3,9,10]. In significance to CRC, it could be stated that the colon epithelium is considered to be in more contact with environmental factors than most tissues as the recipient of dietary intakes, emphasising the needed investigation of this aspect. Moreover, the association between obesity and obesity-related disease such as type 2 diabetes (T2D) to overall cancer risk has been long established [14]. On a molecular level, hyperinsulinaemia or high C-peptide levels has been observed to correlate with malignancies, which partly explains the therapeutic effects observed when using metabolic drugs such as metformin [15] [14].

Specific nutrient consumption could also influence the incidence of CRC epigenetically in the absence ailments. Members of the vitamin B family, namely, folic acid, Riboflavin and cobalamin in addition to the vitamin-like choline are known to regulate chromatin methylation through one-carbon metabolism as they can be donors of their structurally available methyl group [12]. Other examples include DHA, an omega-3 fatty acid which have the capacity to reduce HDAC1 levels *in vitro* thus affecting histone acylation as well as butyrate, short-chain fatty acid spawn in correlation with dietary fibers intake (Fig.1 C) [12].

To conclude, more investigation into the mechanisms connecting nutritional and metabolic aspects with epigenetics and modified gene expression is needed, as understanding their implications on cellular metabolic responses and signal transduction could prove helpful, given the existing possibility of reversing these epigenetic changes;; [9,12,13]. The previously mentioned ties put cellular metabolism in the centrepiece of the crosstalk and a main point of interest to this thesis.

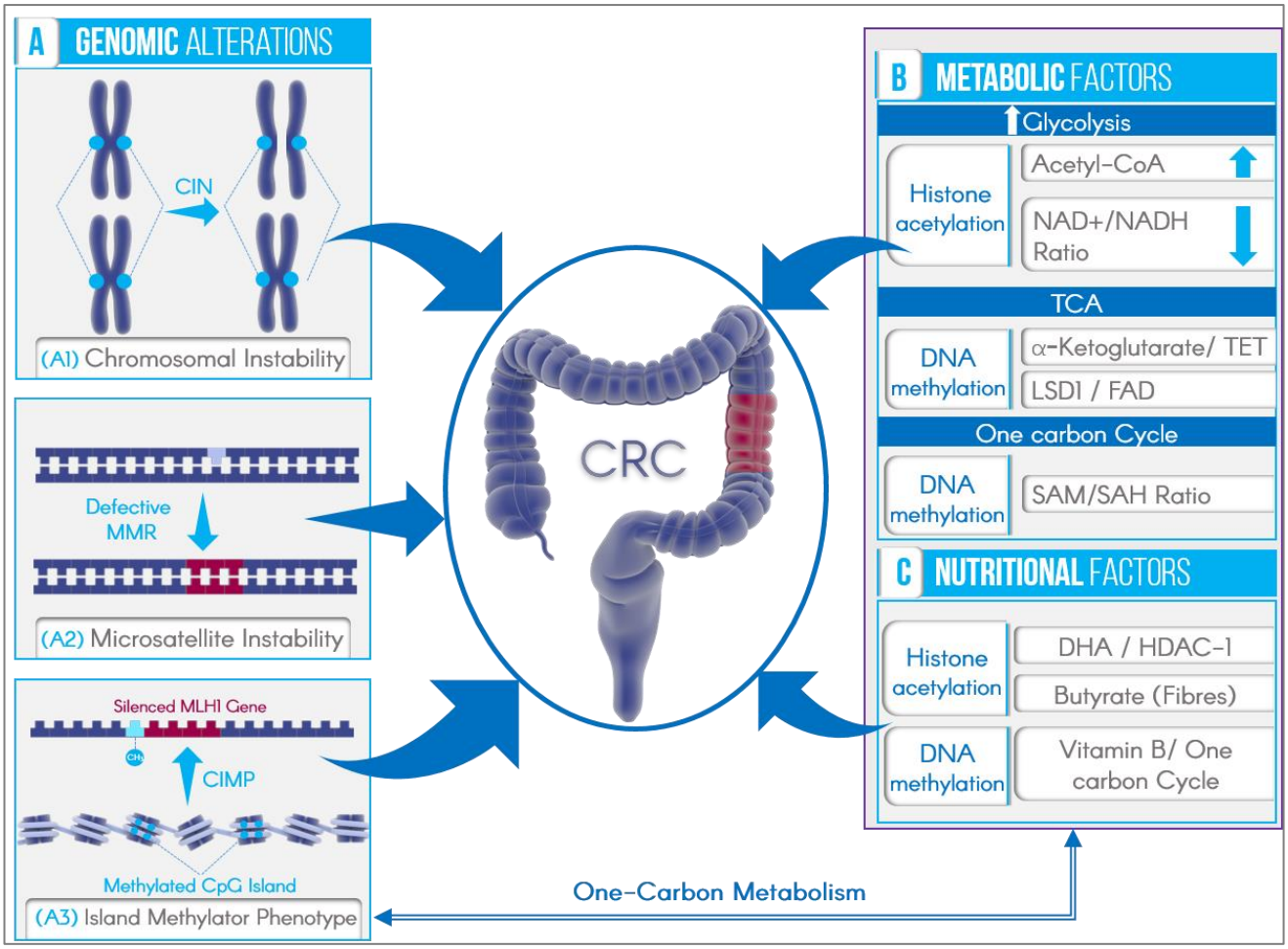

FIGURE 1 *The contribution of various factors into the development of CRC.*

the possible involvement of Metabolic (B) and Nutritional (C) factors in inducing genomic alterations (A). accumulating intermediates of the increased glycolysis in cancer, dysregulated TCA can induce DNA methylation through TET-proteins and FAD mediated co-factored by Lysine-specific histone demethylase 1 (LSD1) and α-Ketoglutarate respectively. One carbon cycle alongside may also induce DNA methylation through changes in the ratio of S-adenosylmethionine to S-adenosylhomocysteine (SAM/SAH). (C) lifestyle choices in diet result in various epigenetic modifications that may contribute to the step-wise development of CRC (e.g. Docosahexaenoic acid (DHA; Omega3 FA) mediated histone acylation by Histone deacetylase 1 (HDAC-1)) by inducing mutation of involved genes.

1.3 CANCER CELL METABOLISM

Understanding the metabolism of cancer cells is a crucial step in uncovering more tools to detect tumour progression, discovering their means of survival facing various stress conditions as they implement multiple metabolic adaptations, and potentially unlocking the secrets to probable therapeutic agents to help fight cancers more efficiently. One of

the more important discoveries in cancer metabolism dates back to 1920s, when the observations of *Otto Warburg* were published in his paper "*The Metabolism of Tumors in the Body*" demonstrated the importance of tracking the altered metabolism of cancer cells, as he first noted the increased accumulation of lactic acid, a currently establish outcome of the hallmark increased glucose transport and consumption [16,17].

This high glucose consumption is explained in what is later known to be the Warburg effect, where cancer cells substitute the original glucose metabolism in which the resulting pyruvate from glycolysis transforms into acetyl-CoA and used inside the mitochondria to generate 36 ATP molecules with aerobic glycolysis producing only 2 ATP molecules even though they have higher energy needs [18,19]. The mentioned change in metabolism is done by exploiting a regulated normally occurring pathway in cells facing insufficient oxygen supply by enforcing various gene deregulations [18,20]. This energetically inefficient utilization of glucose provides cancer cells with the essential metabolites crucial for their rapid growth [16] and occurs more predominately in highly proliferative cancer cells, which are more likely to find themselves in hypoxic conditions as their growth outpace angiogenesis. In response, the cells activate the Hypoxia Inducible Factor (HIF), which in turn promotes glycolysis by upregulating the transcription of several glycolytic genes as well as glucose uptake by increasing the transcription of Glucose transporter 1 (GLUT-1) [17,21]. However, recent studies show that tumours do not fully lose their mitochondrial functions, maintaining the capacity to increase cellular respiration, and therefore sustaining a slow proliferative states to endure chemotherapeutic agents [20, 21].

Extending the knowledge in cancer metabolism unveiled several underlying metabolic adaptations surpasses aerobic glycolysis to overcome stress conditions other than energetic needs. Cancer cells shown the ability to produce NADPH by converting the TCA intermediate, Malate, into pyruvate. The produced NADPH helps in reducing glutathione to increase the tolerance against free radicals. NADPH can be also produced by regulating sterol synthesis via ribosomal protein S6 kinase beta-1 (p70S6K), in a process of which cells oxidize the resulting glucose-6-phosphate from glycolysis in Pentose Phosphate Pathway (PPP), which can be used to accelerate cytosolic lipid synthesis in cooperation with acetyl-CoA [4,16]. The needed acetyl-CoA can be also obtained in the absence of sufficient glucose supply from the glutamine-derived citrate by reductive carboxylation as the former undergoes hydrolysis to form glutamate and equilibrates with α-ketoglutarate in TCA [16].

1.3.1 REGULATORS OF CELL ENERGETICS

As previously mentioned, the mitochondria could play pivotal roles in the survival of cancer cells as they are able to adjust their mitochondria dependency in response to various conditions in their environment. AMP-activated protein kinase (AMPK), a heterotrimeric protein, is one of the first enzymatic tools cancer cells use to fine tune mitochondrial actions. Being regulated by various cellular adenylates and a direct agonist of AMP, AMPK could be activated by the allosteric binding of AMP to its regulatory subunit γ. AMP accumulates due to unmatched ATP consumption in comparison to its production, creating an elevated intracellular AMP/ATP ratio making AMPK an energy sensor that balances mitochondrial content with glucose homeostasis [4,14,22]. As a downstream target of liver kinase B1 (LKB1), Calcium/calmodulin-dependent protein kinase kinase 2 (CamKKb) and TGFβ Activated Kinase 1 (TAK1), AMPK is activated in numerous stress situations depending on the stimulated upstream kinase, and works on ensuring cell survival by engaging several metabolic mechanisms that aims to restore energy balance (Fig.2). Its activation can induce glycolysis, beta-oxidation of fatty acids and autophagy in order to generate ATP. Parallelly, it is able to inhibit protein and lipid synthesis to cut down on ATP consumption. Moreover, by maintaining NADPH levels, it can protect the cells from oxidative damage [22,23].

In tumours, the impaired status of mitochondrial respiration promotes the activation of AMPK. While its wide dynamic responses facing unfavourable microenvironmental conditions undoubtedly aid cancer cell survival and therefore portray AMPK as an obvious oncogene, its inhibition of the *mechanistic target of rapamycin complex 1* (mTORC1) to preserve ATP as a downstream effect of LKB1 by phosphorylating either TSC2 or mTORC1 regulatory subunit Raptor paradoxically hints at some tumour suppression functions. This is further established by that fact that both tumour suppressers TSC2 and p53 fall downstream to its effects [4,14,22,23].

The previously mentioned mTORC1 is one of two distinct complexes forming *mTOR*, a PI3K family kinase seen on the mitochondrial surface, that regulates cell proliferation and protein synthesis. Certain tumours can overexpress mTOR to regain the oxidative phosphorylation energetic efficiency under stress conditions, while its dysfunction in other tumours can promote aerobic glycolysis [20,23].

mTORC1 works in close relation with PI3K–Akt signalling forming a vital pathway (PI3K–Akt–mTOR) to regulate glucose uptake mainly by controlling glucose import using transporters such as GLUT-1 [20,24]. Responses to extracellular stimulators triggers receptor tyrosine kinases (RTKs) and G-protein-coupled receptors (GPCRs) leading to the activation of the lipid kinase PI3K, which in turn phosphorylate PIP2 to PIP3. As PIP3 accumulates within the cytosol, it drives the activation of *pleckstrin homology (PH)* containing molecules by attracting them to the plasma membrane. The downstream mTORC1 gets activated by GTP-activated *Rheb* at the lysosome. In cooperation with *cMyc* (*MYC* oncogene encoded transcription factor), PI3K–Akt–mTOR signalling controls cell proliferation and growth, making it a constant target of dysregulation in cancers [20, 24]. This cascade of events is extensively regulated by multiple mechanisms to cease possible exploitation. The main negative regulators are, PTEN at PI3K level as it reverts accumulated PIP3 to PIP2, GSK-3b at *c-Myc* level by phosphorylation which leads to its degradation, TSC1/2 which negatively regulates Rheb, and S6K1 , a substrate of mTORC1 itself controlling the signal influx and therefore providing a negative feedback to the PI3K–Akt–mTOR pathway [20,24].

Unfortunately, many of these checkpoints are hurdled by oncogenic Akt activity. Akt has the capacity to phosphorylate and therefore inhibit TSC2 and GSK-3b or directly phosphorylate mTOR activating mTORC1 (Fig.2) [24]. Moreover, through Akt/PKB signalling seen in glycolytic phenotype of cancer cells, it can suppress PTEN through NADH accumulation [20,25]. It has been suggested that Akt actions are normally regulated by the second complex of mTOR, mTORC2 which can phosphorylate Akt in what seems to be a modulative tuning between mTORC1 and mTORC2 [20].

To sum up, mTOR dysfunction is a clear promotor of tumorigenesis, together with any damage to the mitochondrial DNA rendering its oxidative phosphorylation defective, as seen in numerous cancer tissues, could cause a shift to aerobic glycolysis "Warburg effect" assisted by Akt/PKB signalling, and provide rationale for this inefficient utilization of glucose besides its benefits on cell growth and overcoming hypoxic stress. As stated, extensive mechanisms keep mTORC1 regulations under check, many of which are closely related to AMPK such as the upstream LKB1, or the downstream, TSC2. Nonetheless, whether we consider AMPK an oncogene or a tumour suppressor, there are no doubts that its dual functionality puts it under the scope for pharmacological targeting of cancer cells [20,23,25].

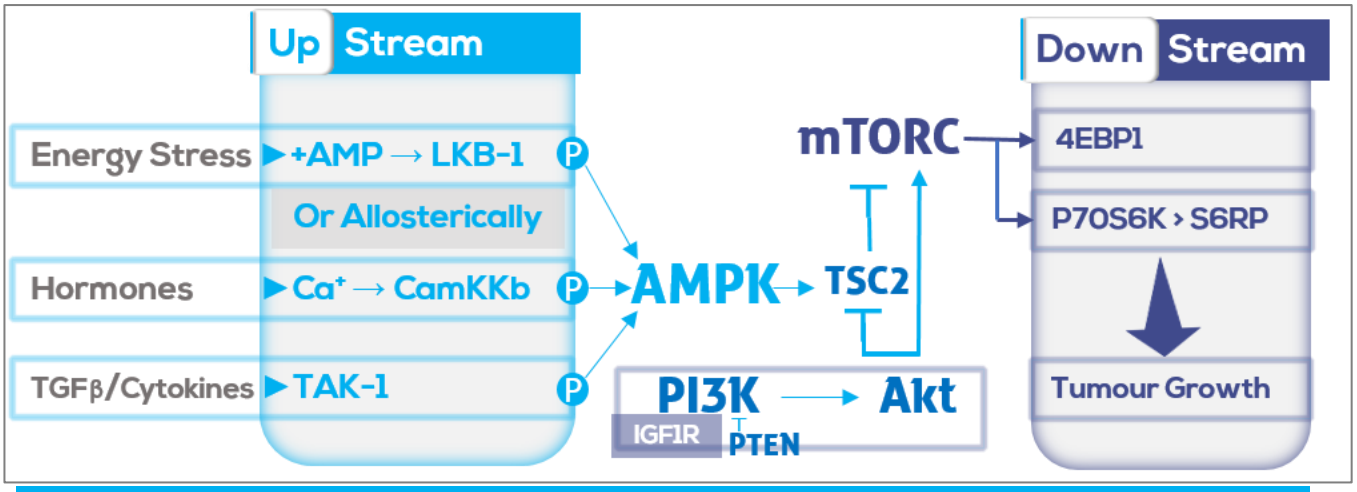

FIGURE 2 *The central role of AMPK in cellular energy modulation.*

A major mode of AMPK action is via its mTORC inhibition which can be countered by Akt signalling. AMPK responds to multiple extracellular signals by a variety of upstream effectors, including hormonal regulation via CamKKb and immunological regulation via TAK-1. It also responds to the cellular AMP/ATP levels to maintain energy homeostasis. The dysregulation of its downstream mTORC can promote tumour growth by its induction of 4EBP1 and P70S6K, a regulator of sterol synthesis and enabler of PPP glucose metabolism in response to stress [4].

Abbreviations used: (LKB-1: liver kinase B1), (CamKKb: calmodulin-dependent protein kinase kinase b), (TAK-1: TGF-b-activated kinase-1), (AMPK: AMP-activated protein kinase), (IGF1R: Insulin-like growth factor 1 receptor precursor), (Akt: Protein kinase B), (TSC2: tuberous sclerosis complex2), (mTORC1: mammalian target of rapamycin complex 1), (4EBP1: translation initiation factor 4E-binding protein 1), (P70S6K: S6 ribosomal protein via p70S6 kinase)(S6RP: Phosphorylated S6 ribosomal protein)

1.3.2 OXIDATIVE PHOSPHORYLATION DYSFUNCTION IN CANCERS

To fully comprehend the rule of mitochondria in cancers, it is important to examine the main energetic pathway occurring within, oxidative phosphorylation (OxPhos). Through TCA cycle, which is tightly coupled to OxPhos, the mitochondria produce the reducing equivalents, NADH and $FADH_2$, mainly from the oxidation of sugars and lipids yielding the necessary electrons to be utilized by a series of mitochondrial inner membrane protein complexes, known as the electron transport (ETC) chain to generate ATP [26,27]. In contrast to the anaerobic conditions, where pyruvate is metabolized to lactate in the absance of oxygen, OxPhos channelled pyruvate is converted to acetyl-CoA after being transported into the mitochondrion, accumulating with each citric acid cycle and

generating NADH (3 molecules) and $FADH_2$ (one molecule). Acetyl CoA can be alternatively yielded in the mitochondria by the oxidation of fatty acids [26,27].

The electrons donated from NADH and $FADH_2$ in the mitochondrial matrix flow with the help of the mobile electron carriers, coenzyme Q (CoQ), through the following series protein complexes with decreasing redox potential: NADH–CoQ reductase (complex I), Succinate–CoQ reductase (complex II), CoQH2–cytochrome c reductase (complex III), Cytochrome C oxidase (complex IV), while the last complex transfers electrons to molecular oxygen reducing it to water. This movement of electrons is coupled to pumping protons by chain complexes from the mitochondrial matrix to the inner membrane generating a proton–motive force across the mitochondrial inner membrane powered by the positive proton concentration gradient and faced by negative electric potential. As the accumulated protons flow back from the intermembrane space through ATP synthase crossing inner mitochondrial membrane into the mitochondrial matrix, they allow it to generate ATP from ADP and phosphate (Fig.3) [26,27]. However, protons could bypass ATP synthase and leak to the mitochondrial matrix uncoupled of proton pumping (uncoupled respiration) mediated by uncoupling proteins (UCPs), part of the mitochondrial inner membrane anion transport carriers (Fig.3) [27]. In the case of UCP1 which is found abundantly in brown adipose tissue, this leak's main function is to produce heat, hence its name, thermogenin. On the other hand, the physiological functions of proton leaks mediated by UCP2, which is expressed in various tissues and UCP3, which is found mainly in skeletal muscle, are still under investigation. Nonetheless, and through loss of functions studies, it has been suggested that they are responsible of limiting the maximal value of the proton gradient [27], in a protective mechanism against oxidative damage caused by the production of superoxide. Therefore, UCP2/3 negatively regulate the membrane potential and ATP production [27,28].

Despite the notion that cancer cells, mainly rely on glycolysis to generate ATP, adapting to survive with an impaired mitochondria, recent studies confirm the ability of tumours to reactivate, even in part, mitochondrial functions [20,29]. As demonstrated in a 2015 study by Lu, Qin et al. tumour cells, under certain stress conditions, can revert their dependency to mitochondria to produce their energy needs by reprogramming their cellular bioenergetics back to mitochondrial respiration in what they described as the "Warburg–Reversing Effect". More specifically, in response to genotoxic stress, cancer cells could

relocate mTOR to the mitochondria allowing its interaction with Hexokinase II (HKII), hence activating OxPhos and increasing mitochondrial ATP production [20].

Observations in epithelial cells lacking mitochondrial DNA (rho$_0$), a cellular model of the Warburg effect, showed an overexpression of UCP2 correlating in cancers with a more aggressive phenotype. The upregulated UCP2 in these tumours uncouples the oxidative phosphorylation by reducing its membrane potential which in turn decreases pyruvate utilization to the mitochondria, therefore, enforcing a dependency on aerobic glycolysis to produce ATP "Warburg effect". This overexpression could be driven by the increasing levels of reactive oxygen species (ROS) in tumours under oxidative stress. Thus, the proposed function of UCP2. is to modulate ROS production, protecting the cell from oxidative damage [28,30.31].

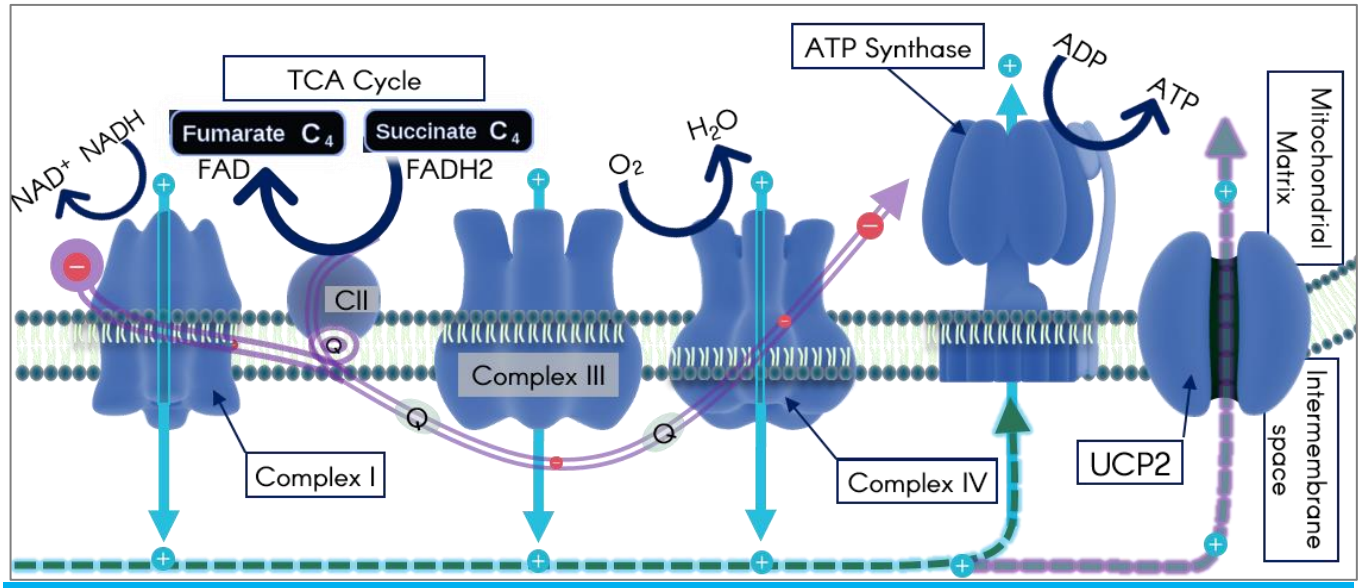

FIGURE 3 *The Electron Transport Chain (ETC) and proton leak event.*

The energy producing proton pump (in cyan) into the intermediate space by membrane bound electron chain complexes is fuelled by TCA intermediates, producing reducing equivalents such as FADH2. To oppose oxidative stress and many cancer cell types, these protons (H^+) are offered an alternative way back to the mitochondrial matrix apart from ATP synthase through UCP2 (in purple), evading the accumulation of ATP and its consequential negative feed-back.

1.3.3 GENETIC IMPLICATIONS OF THE IMPAIRED CELL SIGNALLING AND ALTERED METABOLISM IN CRC.

Most of sporadic CRC progress from a treatable adenoma to a highly developed malignancy through the actions of diversified genetic mutations, dictating the course of the disease with their implications on cell signalling over periods that could take up to 10 years. The discovery of *APC* gene on chromosome 5q.11, which was later found to have an acquired mutation in almost 90% of colorectal neoplasms, was an important opening to the unveiling of many of these mutations, several were found to be unique to CRC (i.e. chromosomal deletions on 17p 18q and 5q) [3] [6]. The importance of APC as a tumour suppressor emerge from its regulating effects on β-catenin by promoting its GSK-3β-triggered ubiquitination as part of the multiprotein complex of APC, Wtx and Axin. In the absence of APC, increased concentrations of β-catenin can upregulate the transcription of c-myc (amplified in 30% of CRC), triggering its proliferative actions on a cellular level and resulting in stem cell-like undifferentiated cells forming the adenoma. The previous process happens in cooperation with Wnt signalling that can further inhibit GSK-3β actions [5,6,32]. Mechanisms involving PDK1 have been identified demonstrating Wnt signalling engagement in the acquisition of Warburg phenotype [33].

One of the main driving factors to the uncontrolled proliferation of cancer cells is the constant triggering of growth factor receptors, mainly epidermal growth factor receptor (EGFR). The fact that EGFR acquires a mutation in less of 5% cases of CRC is downplayed by the high mutation rate of its downstream oncogene *KRAS*, in 40% of CRC [5]. The mutational degree of the extracellular growth signals transmitter protein encoded by *KRAS* holds a special significance due to its correlation with increased adenomas lesion size (14% in adenomas smaller than 2 cm 33% in ones bigger than 2cm and up to 50% is highly dysplastic lesions) [5,6].

Another downstream of EGFR, Governing nutrient uptake, is the phosphoinositide 3-kinase (PI3K) pathway, one of the most dysregulated in cancers through mutations in its different components, and especially in CRC. In up to 30% of CRC, a somatic mutation in PIK3CA, which encodes the PI3K catalytic subunit, is found and predicts less effectiveness of EGFR inhibitors. Mutations in PIK3CA may happen along with *KRAS* mutations in contrast to *BRAF*, but does not require it. Another main mutational mechanism is targeting the pathway's regulator and tumour suppressor, PTEN, in 10% of

sporadic CRCs. Similarly, PI3K's inhibitory subunit, encoded by PIK3R1 gene suffers from mutations in 4% of CRCs. [5,10].

1.4 THE VALUE OF BIOMARKERS IN CRC.

CRC is more common in older populations, rendering many of its clinical manifestations like fatigue, weight loss and shortness of breath to have very little diagnostic value. Therefore, it is important to discover non-invasive screening process through molecular detection to replace colonoscopy able to analyse batch samples and more accepted by patients. Faecal DNA tests for APC and KRAS mutations are able to detect CRC with fair sensitive [3]. Nonetheless, the potential of metabolic biomarkers could prove more useful in identifying the energetic phenotype of cancer and therefore direct the use of appropriate therapeutic agents.

1.4.1 BIOMARKERS OF INTEREST IN CRC METABOLIC INTERPRETATION AND DIAGNOSIS

Glucose is imported into the cells by 2 families of hexose transporters, GLUT and SGLT. 14 isoforms of GLUT are expressed in a tissue-specific pattern across cellular membranes controlling its glucose metabolism [17,19,34]. GLUT-1 is of a special interest as the most widely expressed isoform meditating glucose uptake and found abundantly expressed is many tumours [5,17]. The increased glycolysis imposes the facilitation of glucose uptake to the cell. Therefore, cancer cells appear to alter GLUT-1 expression levels in correlation with increased hypoxic stress. The AKT induced activation of mTORC1 upregulates the HIF1α-dependent transcription of GLUT-1 mRNA, which is further positively upregulated by the consequential increase of c-Myc [5,19]. Elevated levels of GLUT-1 mRNA is found to be significantly high in Right-sided colon tumours [4].

The dysregulated GLUT-1 expression levels were first used as a marker for infantile skin hemangioma, and it is currently under investigation as a prognostic indicator. GLUT-1 correlation with tumour detectability by PET also gives it a diagnostic value. Despite the current poor understanding of its metabolic implications, there is a clinical significance that comes from the correlation between higher expression GLUT-1 with tumour aggressiveness, dedifferentiation and poor prognosis as it aids in accelerating growth by depriving the surrounding the stroma [17,18,19].

With respect to the enzymatic regulation of glucose metabolism, comes the PDK family which can also be induced by HIF1. PDKs are known to control glycolysis by opposing PDCs actions through their capacity to sense the accumulation of mitochondrial energy indicators, namely, acetyl-CoA, NADH, and ATP [35]. PDK2 has caught more attention as the most expressed isoenzyme of PDKs. Its expression has been linked to increased proliferation in cancers, proven by dichloroacetate (DCA) inhibition, a pyruvate analogue that seemed to be able to halt the proliferation. Physiologically, Insulin is capable of repressing the expression of PDK2 via the phosphorylation of FOXO through PI3K/Akt signalling pathway [35,36].

UCP2, an uncoupling protein homologue that mediates mitochondrial proton leak and linked to the pathogenesis of T2D, is another prospect. It has been proposed that UCP2 regulates superosixide and its downstream ROS in a negative feedback loop. The activation of UCP2 is predictably triggered by superoxides, correlating in production with increased mitochondrial membrane potential. UCP2-mediated proton leak decreases the membrane potential rendering less production of superoxides [27,28]. Elevated UCP-2 expression could be justified as a protective strategy in a Warburg phenotypic metabolism against the high production of ROS by a defective mitochondrion. Therefore, it could be an indicator for this phenotype and a potential therapeutic target [27,28].

1.5 THERAPEUTIC AGENTS

The constant efforts put into finding better screening tools for CRC is an expected response to the unsatisfactory outcomes in regards of long term survival when it comes to developed cases. The incorporation of Adjuvant and Neoadjuvant treatments have increased the chances of a successful resection of the tumour, but did not prove helpful in metastasized CRC [3]. The current adjuvant treatment strategy for stage III CRC is a combination of 5-fluorouracil and oxaliplatin. Whereas the introduction of targeted therapies in the shape of monoclonal antibodies towards EGFR (panitumumab and cetuximab) or VEGF (Bevacizumab) have indeed increased the overall survival for metastatic cases up to 24 months, it has only proven effective in up to 30% of KRAS wild type profiled patients in case of EGFR, stressing the need for a better personalized medicine [9,37]. However, prospects targeting the molecular mechanisms involved in carcinogenesis are currently under investigation, such as the use of UCP2 inhibitors and NSAIDs.

UCP2 can be inhibited directly with the use of Genipin and chromane or indirectly by reducing the superoxide and lipid peroxidation products required for its activation by Vitamin E. Still, neither approaches showed clinical viability to date [30,31]. On the other hand, the widely used Non-steroidal anti-inflammatory drugs (NSAIDs) have showed an anti-neoplastic effect correlated with decreased overall mortalities in CRC via their inhibition of COX protein activity. COX-2, a mediator to the biosynthesis of the proliferation and angiogenesis inducing-PGE2 was found to be overexpressed in up to 50% of colorectal adenomas and 86 % of CRCs [5,9,30]. One NSAID, Sulindacm had the capacity to downregulate WNT signalling by inhibiting β-catenin expression and therefore, induce apoptosis in CRC. In addition to Celecoxib, it also interfered with PI3K/PTEN/AKT signalling to further inhibit angiogenesis. This prospect was also suspended due to increased cardiovascular mortality in trials [5].

The leading obstacle that appears to face the majority of newly approved therapeutic agents is the prompt chemo resistance that stands in the way of decreasing the overall mortalities. The existence of a CSCs derived subpopulation of tumour cells possessing altered metabolism, which endures stress and cytotoxicity, termed chemo-resistant cancer cells (CCCs), is argued to be the main reason for chemo resistance [15,21].

In the absence of cytotoxic agents, most tumours tend to sideline the mitochondria to induce proliferation and to evade its regulatory pathways that could lead to apoptosis granted that it accommodates cytochrome c, one of the most important proapoptotic proteins. Maintaining a defective OxPhos appears to be the main mechanism executed by these tumours to protect them and thrive their growth [29]. Intriguingly, a proposed explanation for the resistance in tumours lies in adopting a metabolic strategy exhibits increased dependency on the mitochondria. Observations from radiation resistance disclosed a deviation from glycolysis towards mitochondrial oxidative respiration to generate the needed ATP by relocating mTOR to the mitochondria which felicitates its interaction with hexokinase II [20]. On the same note, investigating drug resistant tumours unveiled the same shift towards oxidative metabolism [21]. Several studies have indicated that targeting ETC, the engine of oxidative metabolism with metformin (argued to be a complex I inhibitor) results in a selective cytotoxicity towards CSCs and their CCCs derivatives preventing tumour relapse [21].

1.5.1 METFORMIN USE IN CANCER TREATMENT

This thesis's drug of interest, metformin was first synthesized by K. Slotta from galegine, an isoprenyl guanidine extracted from *Galega officinalis* which was used in traditional medicine to treat *diabetes mellitus*. The toxicity of Guanidines was greatly reduced by bonding two of its molecules to form biguanide which was further developed to give metformin [16,38]. Regarded as a first first-line treatment for T2D with prescriptions handed to more than 100 million patients, the exact molecular mechanisms for metformin is yet to be totally understood. Its ability to increase the cellular sensitivity to insulin leads to lowering blood glucose levels without the risk of hypoglycaemia, hence its classification as an antihyperglycemic agent in contrast to sulfonylureas that induce insulin secretion by affecting the pancreas directly [14,16].

The anti-diabetic activity of Metformin is characterised by its ability to oppose gluconeogenesis in an AMPK-independent mechanism. A decrease in hepatic ATP production by disturbing ETC, is thought to equilibrate the enzymatic levels of pyruvate carboxylase, phosphoenolpyruvate and pyruvate kinase ultimately leading to a decreased hepatic glucose production [14,39]. This demonstrates metformin's cellular energy regulating powers that could be useful to apply in cancer cells.

The use of biguanides in cancers dates back to 1971, demonstrating positive outcomes when complimented with a low calorie diet by Dilman [40]. The developed derivative, metformin caught attention after the publication of Evans case-control study in 2005 surveying 12000 T2D patients. Evans confirmed the anti-neoplastic effects of metformin, correlating the observed decline in cancer incidence with increased metformin exposure [14,41]. Moreover, the increasing numbers of metformin users since its FDA approval in 1994 provides retrospective studies with an abundance of epidemiological data. Further meta-analysis indicates that metformin could have a preventive anti-cancer effects seen by reduced tumour incidence by 31% and its associated mortalities by 34% in T2D patients [15,16,42].

1.5.1.1 PHARMACOKINETICS OF METFORMIN

Some of the pharmacological features of metformin have gained it a great appeal for testing in oncology. Exhibiting a well-known toxicity profile, where gastrointestinal discomfort is the main complication and lactic acidosis is quite unlikely in therapeutic

doses under 2.5mg/L is an important driving factor [15, 38, 43]. Put together with the absence of reports about drug interactions during years of co-administration with cancer medication has pushed its clinical evaluation directly into phases II and III [38]. The firm pharmacokinetical knowledge encircling metformin has contributed in better understanding the extent of its biological effects. Its acid dissociation constant (pKa) of 11.5 indicates a low lipophilicity at the blood's physiological pH, as it will be mostly found as an organic cation. This parameter renders the possibility of metformin passively diffusing into the cell very slim [16, 38].

The organic cation transporters (OCTs), mainly OCT-1 and OCT-2 actively transport this positively charged drug into the cells, making them and their polymorphisms a determining factor in metformin's distribution and cellular uptake that seem to show unequal response in around 30% of patients, not to mention that the tissue-specific expression levels of OCTs indicate the cellular accumulation of metformin and the organ sensitivity to its anti-tumour effects [14, 15, 38].

Oral administration of metformin can achieve a bioavailability around 55% and its maximum plasma concentrations is reached after 3 hours. Absorption occurs mainly in the proximal small intestine via plasma membrane monoamine transporter (PMAT) in a pH dependent manner, rendering its stomach and large intestine absorption negligible [38,44]. Metabolically, metformin seems to have a high liver accumulation, but remains unmetabolized with inconsequential binding to plasma proteins during its 6 hours half-life until urinary elimination [16, 38].

1.5.2 METFORMIN'S DUAL MODES OF ACTION

Classification. Multiple pathways has been proposed to explain the pleiotropic anti-tumorigeneses effects of Metformin which can be generally classified into systematic (indirect) and cellular (direct) effects, a clear identification of these pathways recognizing their collaborative and unique mechanisms is thought to be vital to optimize the use of metformin according the cancer metabolic profile [15,42].

Systematic affects (Fig.4 A). The systematic anticancer effects of metformin arise from its general alterations to the body metabolism via the regulation of glucose and insulin levels, known mediators for obesity-associated cancers including CRC [15,42]. As an

antidiabetic agent, metformin enhances glycemic control by inhibiting gluconeogenesis and inducing muscular glucose uptake, therefore affecting the hallmark increased glucose consumption of cancer cells. In addition, its insulin's lowering and sensitizing effects, reduce the mitogenic risks of insulin-like growth factor 1 (IGF-1), as well as its the indirect inhibition of IR-A legend binding an upstream of PI3K/ AKT/mTOR pathway [14, 15, 42]. Using genetically manipulated tumour mouse models, an insulin-independent pathway thought to be through LKB1/AMPK has been observed in which metformin can control cell proliferation [14].

Before going into the specific molecular mechanism in which Metformin affects AMPK, it is worth mentioning that metformin can also reduce the absorption of glucose from the gastric tract by regulating glucose transporters SGLT-1 and GLUT2 [44]. Furthermore, metformin is associated with a reduction of inflammation in the microenvironment of cancers affecting its progression [14].

Direct effects. In the absence of a commonly agreed molecular target of metformin, pharmacological studies investigating its actions indicated a close relation with the activation of AMPK , a commonly dysregulated protein kinase in metabolic syndrome that could lead to the development of CRC. The main perk of AMPK's activation by metformin is the consequent inhibition of mTOR, which is widely upregulated in cancers [42, 43, 45]. Nonetheless, the way in which metformin affects AMPK withstood a long debate. Multiple studies suggest that its activation is resultant to metformin's inhibitory effects on the respiratory chain complex I which in turn reduces ATP levels in comparison to AMP driving AMPK intervention. This mechanism was further established by observing the drug effects in liver-specific AMPK-deficient mice. Other studies have demonstrated the need for LKB1 and ATM (both lying upstream of AMPK) to mediate the cellular effects of metformin (Fig 4B) [14,15,22]. An AMPK independent inhibition of mTORC1 by metformin was also proposed to occur through RAG GTPase pathway. Moreover, a suppression of human epidermal growth factor receptor 2 (HER2) is also thought to be possible by the direct inhibitory effects of metformin on S6K1, a downstream effector of mTORC1 (Fig 4C) [14,15].

Mitochondrial actions. Cell free assay has confirmed that metformin does not trigger the direct phosphorylation of either LKB1 or AMPK, and the activation comes consequently to metformin's mitochondrial effects on ETC. this positively charged drug accumulates

cellularly in the mitochondrial matrix facing the normally occurring proton-motive forces along the inner membrane [14,46]. Its effect on ETC is best described as "a mild and transient inhibition of complex I" decreasing the conversion to ATP from AMP and resulting in an accumulation of the latter which in turn activates 5'-AMP-activated protein kinase allosterically [14,21,42]. When compared to rotenone, a reference complex I inhibitor, the singularity of metformin was demonstrated through significantly less inhibitory powers, suggesting a probable difference in the distressed complex I subunit. Additionally, metformin exhibit a unique ability to selectively block complex I reverse electron flow, decreasing ROS production [14]. Another probable site of action is the mitochondrial glycerophosphate dehydrogenase (mGPD), when considered together with complex I inhibition, metformin accomplishes a high level of disturbance to the entry of reducing equivalents via glycerol-phosphate shuttle that would further implicate the mitochondrial oxidization of cytosolic NADH [42].

The current main attraction for using metformin in cancer therapy is its ability to affect the stem-like cancer cells (CSC) sub-population in cancers which are thought to be responsible of tumour relapse. By targeting OxPhos dependent cells including CSC and CCC, metformin has established the ability to abrogate cancer relapse when used with a chemotherapeutic agent able to induce a shift towards OxPhos or unable to eliminate these resistant cells [15,21]. These observation has been seen clinically in 5-FU-resistant colon cancer cells [21] and *in vitro* by confirming the absence of the stem cell marker signature CD44C/CD24lo [15].

Regulation of Lipogenesis. The *de novo* synthesis of fatty acids (FA) is a known phenomenon that thrives the progression of cancers (including CRC) via the overexpression of Fatty acid synthase (FAS) and Acetyl-CoA carboxylase (ACC). Metformin has demonstrated the ability to regulate FAS on a transcriptional level by inhibiting SREBP-1 mediated by AMPK activation. It can also promote the inhibitory phosphorylation of Acetyl-CoA carboxylase (ACC) resulting in a growth reduction in some cancer phenotypes [14,16].

Metformin, P53 and epigenetic modifications. The guardian of the genome, P53, is an inevitable player in almost every cancer's progression or prevention. In the context of colon cancer, it has been observed that metformin may induce apoptosis in CRC in by reducing the upregulated glycolysis and autophagy due to a dysfunctional p53 as a result of

nutrient deprivation. *In vitro*, metformin inhibited p53-deficient colon carcinoma growth. Interestingly, P53 might play part in sensitivity to metformin particularly in colon carcinoma apart from other cell lines [14,15]. However, the exact way in which metformin affects P53 remains to be elusive. Its interactions of TCA cycle, which changes cellular acetyl-CoA levels are thought to a play part in reducing the acetylation of p53 epigenetically mediated by histone deacetylase SIRT1 [47]. Yet, low metformin concentrations shown to increase p53 acetylation, a process thought to be important for its tumour suppression properties [47, 48]. In a more general spectrum, by influencing the production of TCA-cycle intermediates such as acetyl-CoA and αKG, Metformin is able to influence the epigenetic changes exerted by these co-factors in a still unclear mechanisms [47].

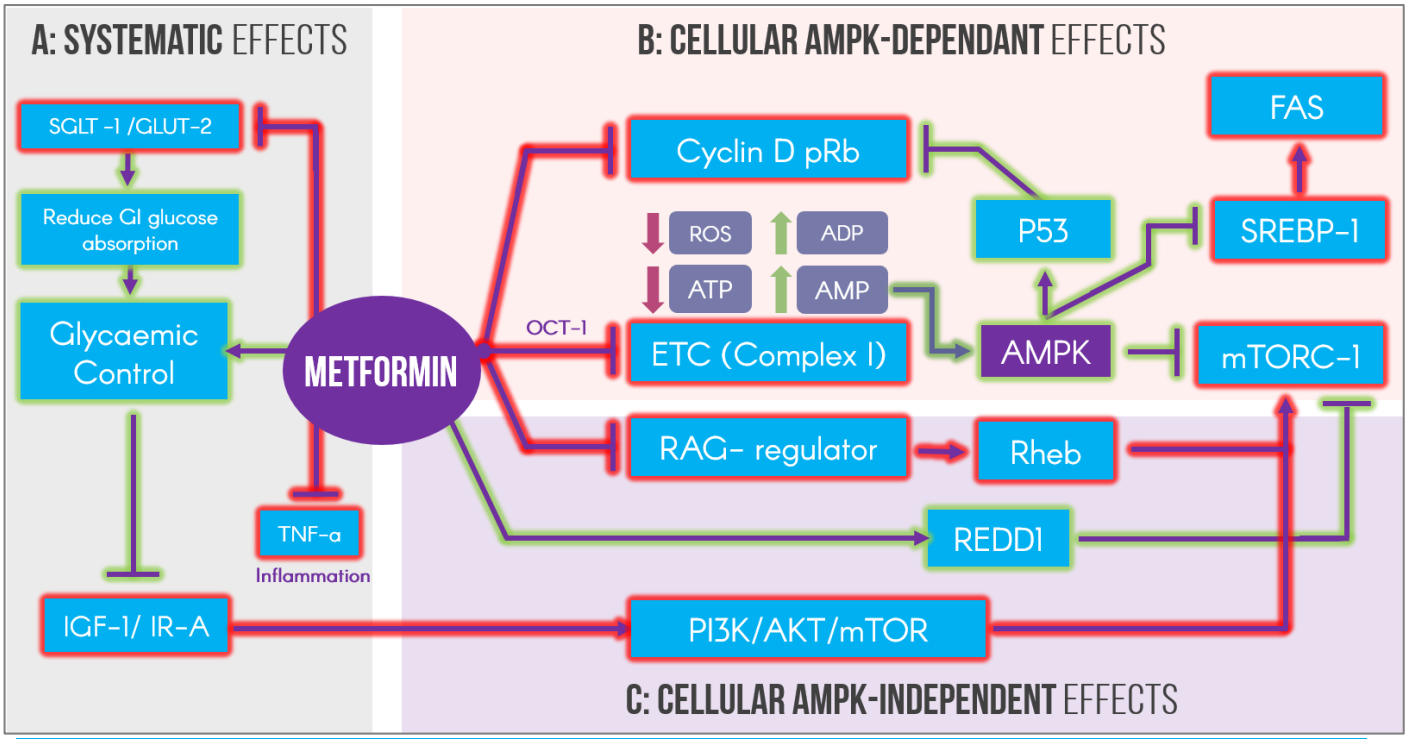

FIGURE 4 *Metformin's systemic and cellular effects.*

Multiple pathways are involved in metformin actions. Its systemic effects (A) are mainly due to regulating blood glucose levels (grey box), by modulating the transporters responsible of its absorption and increasing the peripheral sensitivity to insulin, ultimately lowering the later plasma levels and its subsequent IR-A mediated PI3K pathway activation. Alongside that, metformin can exert its effects directly on a cellular level through AMPK-dependent (B) or AMPK-independent mechanisms (C) to inhibit mTORC-1, it also may regulate fatty acid synthesis (FAS) via SREBP TFs and promote P53 by activating AMPK. Metformin REDD-1 (regulated during development and DNA damage responses 1) mediated effects are explained in other literature [16].

CHAPTER 2. RESEARCH AIMS AND HYPOTHESIS

2.1 RATIONALE

The extended debate concerning the use of metformin in cancer has resulted in varying arguments over the years, most conducted studies argue its use as either a preventive or adjuvant agent [43]. Moreover, retrospective studies depending on the immense availability of data derived from its use in diabetics were inconsistent in terms of results. Some noted no significant effects on the development of some cancers [43], others have associated it with the development of cancers in T2D patients [15]. Even though meta-analysis of retrospective studies has reported a 31% overall reduction in cancer indicant, it is worth noting that these results are observed in T2D patients which do not necessarily reflect the metabolic status of non-diabetics [15]. In that context, the improved insulin sensitivity after metformin treatment appears to be firmly associated with diet. Studies in mice demonstrated a decline in IR-mediated tumour progression when on high energy regimen in contrast to a growth inhibition in controls [15]. Nonetheless, retrospective cohort studies assessing an approximate of 25,000 patients have demonstrated that the use of metformin is advantageous in CRC [43].

The use of metformin to treat diabetes, a metabolic disease, for decades due its metabolic altering actions is a solid reason to evaluate its use in cancer on a metabolic basis as well, which is not widely the case as of now. On the one hand, ongoing *in vitro* studies have tested metformin's effects mainly on cell-lines cultured in proliferation promoting media that contains an excessive supply of growth factors and glucose (2-5 folds the physiological levels) [15]. These levels do not reflect the physiological scenarios in the body, as this abundance of glucose is expected to weaken the urgency for a shift towards mitochondrial dependency where metformin is expected to act. This is extremely important when metformin is used an adjuvant treatment alongside a chemo therapeutic agent that would most likely derive an OxPhos energy reliance [43]. On the other hand, the assessment of metformin *in vitro* has been carried on using a wide range of concentrations, (1-40mM) many of which are not feasible clinically [15]. For example, a one forth delay in tumour onset achieved by using 300mg/kg is hardly impactful as its tenfold higher than the therapeutic window. On the other hand, a recent study showed that 10mM concentrations (achievable *in vivo*) have shown to be effective in reducing tumour growth [15].

To address the previous points, metformin is to be evaluated in this thesis regarding the metabolic profile of the cell line in use, and the consequent underlying preferred pathways that would heavily impact metformin's effects. Up until now, the author is not aware of any publication addressing metformin's benefits in regard to metabolic profiles which emphasise the need for this research.

2.2 SPECIFIC AIMS

This study was conducted to evaluate the actions of metformin on a highly glycolytic cancer cells; SW948, in the absence of any interfering chemotherapeutic agents. The assessment is made with respect to viability, mitochondrial content, and GLUT-1 regulation as a marker on both transcription and expression levels. The final remarks would consider a sister study conducted also at CORE that would assess metformin in an OxPhos dependent cell lines representing a shifted energy dependency.

2.2.1 CHARACTERISTICS OF SW948 CELL LINE

SW948 are established to be a highly glycolytic cell-line through previous unpublished work from research group leader and thesis supervisor, Hanne Hagland.

TABLE 1 Features and Genetic Characteristics of in use SW948 cell-line

ASPECT	STATUS	NOTES	REFERENCE
MAIN FEATURES			
ORIGIN	Grade III adenocarcinoma	Obtained from the colon of an 81-year-old Caucasian female	[7, 8, 49]
MORPHOLOGY	Epithelial		[50]
GENETIC MUTATION PATHWAYS			
MSI STATUS	MSS	Stable	[8]
CIMP PANEL	Negative	-	[8]
CIN	Positive	-	[8]
SPECIFIC GENES			
KRAS	Mutated	Heterozygous alleles Missense mutation: Q61L; CAA>CTA	[8, 50]
BRAF	WT	-	[8]
PIK3CA	Mutated	homozygous alleles Codon: E542L; GAA>AAA	[8, 51]
PTEN	WT	-	[8]
TP53	Mutated	homozygous alleles	[8]

		Codon: G117fs; GGG>GG	
APC	Mutated	Nonsense mutation; c.4285C>T |	[50]
SMAD4	Mutated	Missense mutation; c.1609G>T	[50]
OTHER GENES	Mutated	c-Myc, H-Ras, N-Ras, myb and fos	[50, 52]

2.2.2 IN VITRO APPROACH

Aims:

- Evaluate the effect of metformin on highly glycolytic cancer cells.
- Determine if Glut-1 is an indicator of energy shift.
- Estimate mitochondrial changes in response to metformin.
- Investigate genetic changes to locate metabolic biomarkers and compare transcription levels with expression levels of metformin.
- Identify the likelihood of metformin effectiveness.

2.3 RESEARCH IMPACT

If metformin proved to act differently in highly glycolytic cancer cells than it does in OxPhos dependent cancer cells that would provide evidence for a targeted mechanism in tumours which promotes its use as an adjuvant drug to prevent cancer relapse especially in combination with other chemo therapeutic drugs to activate its chemo sensitizing potential within clinical doses. The insights obtained from comparing physiological glucose culturing medium to the proliferative high in glucose medium are aimed to provide grounds for future *in vitro* research emphasising on the importance of this aspect in assessing metformin's effectiveness in relation to the metabolic situation.

CHAPTER 3. METHODS

3.1 CELL LINE AND CELL CULTURE

SW948, a human colon carcinoma cell line, originally established in Leibovitz laboratories [49] and purchased from Sigma[1*], were passed routinely in 75 cm^2 tissue culture flasks[2] using high glucose DMEM medium[3], supplemented with 10% fetal bovine serum (FBS), 2mM/l (0.584 g/l) L-glutamine, penicillin (100 U/ml) and streptomycin (100 µg/ml). The cells were constantly incubated at 37°C under 5% CO_2[4] to 50-70% confluence before use in various assays.

3.1.1 DIFFERENTIAL CULTURING CONDITIONS:

In the prospect of establishing an improved understanding of the actual responses mediated by SW948 cell line, a twosome of culturing mediums has been used parallelly in all the performed experiments to follow:

A. High Glucose Culture Medium[3]: The routine medium containing high glucose levels of 4.5 g/L which is used to grow and pass the cells is always present in the first set of cultured samples (HG set), including an independent high glucose control and treatments for 24 and 48 hour intervals unless otherwise stated. Specimens cultured using this medium to represent the most commonly used culture condition in other studies and will be regularly investigated side by side to the second set.

B. Physiological Glucose Culture Medium: GlutaMax-I DMEM[4] containing physiological glucose levels of 1 g/L, supplemented with 10% FBS, penicillin (100 U/ml) and streptomycin (100 µg/ml), was used to grow the second set of cultured samples (LG set), with an aim to reproduce a similar environment to the one present clinically. This set also compiles of its own Physiological Glucose control and treatments for 24 and 48 hour intervals unless otherwise stated.

3.2 MANUAL PROLIFERATION ASSAY UNDER DIFFERENTIAL CULTURING CONDITIONS

To assess proliferation profile and doubling times, 1×10^4 SW948 cells were seeded in 6-well plates[5] with the addition of 3 ml of high and physiological glucose culturing mediums

* Detailed information about the used products as indicated ›are found in the appendix table.4

(as indicated in 3.2.1.1). The cultures were incubated at 37°C for a total of 72 hours, and cell viability readings were taken at intervals of 6, 12, 24, 48, and 72 hours. After each incubation period, the medium was removed by aspiration for each well separately at its indicated time interval, and the cells were washed in Dulbecco's phosphate buffered saline[6] to prepare them for trypsinization with 0.5 ml of Trypsin–EDTA[7](0.25%) in order to count the viable cells. The trypsinization process was halted using 1.5 ml of the corresponding growth medium, and the cells were moved to Eppendorf tubes for counting. A 100 µL of trypan blue[8] was added to a 100 µL homogenized solution of the extracted cells (1:1 v/v) in pursuance of differentiating the viable cells from the necrotic ones, and then loaded to the hemocytometer[9]. Three distinct replicates were performed using SW948 cell passages 12,15, and 16 respectively, the average cell count in different glucose concentrations was compared over time intervals and plotted exponentially to determine the growth rate and calculate doubling time as in: $\frac{\ln 2}{\text{growth rate}}$

3.3 MTS CELL VIABILITY ASSAY

To determine the effects of the metformin treatment on cell growth, MTS cell proliferation assay has been conducted. SW948 Cells were cultured to 50% confluence, harvested and counted. HG and LG sample sets of SW948 cells (as indicated in 3.2.1.1) were plated in three technical replicates at 1.0×10^4 cells/well in a pair of 96–well culture plates[10] and incubated at 37°C with 5% CO_2 for 24 hours to allow attachment after the addition of 200 µL of high and physiological culture medium to each of the corresponding sets. After 24 hours of attachment time, the wells were replenished with fresh corresponding mediums encompassing metformin[11] at various concentrations. Five series of metformin dilutions, 0.1mM, 0.5mM, 1mM, 3mM and 5mM, in high and physiological culture mediums have been prepared and added to the matching well triplicates, maintaining a volume of 200 µL in each well. One set of replicates for each set (HG set, and LG set) was left as a control (untreated) and blank wells were instilled with the corresponding medium exclusively, to subtract background readings.

After an incubated treatment period of 20 hours, 20 µL MTS reagent[12] was added to each well in the 24 hours' plate and incubated again for an extra 4 hours. A subsequent 96 wells plate was incubated for a treatment period of 44 hours before adding 20 µL MTS reagent for 4 hours to prepare it for optical density (OD) reading.

3.3.1 UNIFORM SAMPLE SETTINGS

Depending on the results obtained from MTS assay that demonstrates the most effective metformin concentrations, 0.5mM/L, 3mM/L metformin treatments have been selected for further investigation. The emerging specimen model comprises the following 10 sample variations:

TABLE 2 Experimental Sample Design

	HG SET		LG SET	
CONTROLS	I: High Glucose Untreated Control		VI: physiological Glucose Untreated Control	
24-HOUR TREATMENTS	II: High Glucose 24hrs, 0.5mM metformin Treatment	III: High Glucose 24hrs, 3mM metformin Treatment	VII: physiological Glucose 24hrs, 0.5mM metformin Treatment	VIII: physiological Glucose 24hrs, 3mM metformin Treatment
	This set was incubated for an extra 24 hours to eliminate effects that could arise from different medium exposure times and confluency levels, and therefore resulting in common control sets			
48-HOUR TREATMENTS	IV: High Glucose 48hrs, 0.5mM metformin Treatment	V: High Glucose 48hrs, 3mM metformin Treatment	IX: physiological Glucose 48hrs, 0.5mM metformin Treatment	X: physiological Glucose 48hrs, 3mM metformin Treatment

3.4 GLUT-1 PROTEIN ISOLATION AND IMMUNOBLOTTING

3.4.1 PREPARATION OF PROTEIN LYSATES

SW948 cells were seeded in 6 well plates (1.0×10^6/well) and incubated at 37°C with 5% CO2 for 24 hours to allow attachment in 3 ml of both high and physiological glucose culture mediums (see 3.2.1.1). The culture medium was then aspirated and the cells were treated with selected concentrations of metformin (0.5mM and 3 mM) building upon the MTS assay results, constituting 4 treatments for each culturing medium in addition to a corresponding control (as described in **3.2.3.1**). After a treatment period with metformin

(24hrs, 48hrs), the wells were washed with PBS one more time, trypsinized*, and the cells were harvested into tubes to be centrifuged[13] for 5 mins at 900 rpm and 4°C in order to remove the medium and resuspend the cell pellets in RIBA buffer[15] at 500ml per 1 million cell ratios with the addition of 10 µL of protease inhibitor[16] for every 1ml of RIPA buffer used. Then the cell suspension was centrifuged for additional 5 minutes at 40000 rpm and 4°C. The resulting supernatant containing total proteins were stored into separate Eppendorf tubes (following the previously stated set up in 3.2.3.1) at -20°C.

3.4.2 DETERMINATION OF TOTAL PROTEIN CONCENTRATIONS, SDS GEL AND WESTERN BLOTTING

Protein concentration determination was carried on for each sample individually using BCA method[17] according to the manufacturer's instructions [53]. Equal amounts of protein (10 µg During the first biological replicates, and 7ug during the second biological replicates) were loaded on 12% sodium dodecyl sulphate-polyacrylamide gel electrophoresis (SDS-PAGE) Stain-free gels[18]. The first well was reserved to load a mixture of 5 µL pre-stained Protein ladder[19] and 3 µL magic marker[20]. Electrophoresis was carried on for 90 minutes at 100 voltage using BioRad PowerPac basic[21], and the proteins were transferred thereafter to methanol activated polyvinylidene difluoride membranes using BioRad Criterion blotter[22] for 80 minutes at constant 100 Voltage.
The membranes were blocked with 5% non-fat milk[23] in TBS-Tween[24] 0.1% for 2 hours, followed by overnight incubation at 4c with GLUT-1 primary Antibody[25]. After washing in TBST, the membranes were incubated for 2 hours at room temperature with an HRP conjugated secondary Antibody[26]. After a subsequent wash, 1.5ml of ECL Western Blotting peroxidase substrate for enhanced chemiluminescence (ECL)[27] were added to the Immunoblots for approximately 1 minute, preparing them for visualization using BioRad ChemiDoc™ Touch Imaging System[28]. The GLUT-1 Band intensities were quantified relatively for each sample to its control using the Image lab software (Bio-Rad)[29].

* A subsequent biological duplicate was harvested on ice using cell scrapers[14] directly in RIPA buffer without the addition of Trypsin to inspect any effects trypsinization could have on GLUT-1 Values.

3.5 IMMUNOSTAINING

3.5.1 GLUT-1 IMMUNOFLUORESCENCE AND CONFOCAL IMAGING

SW948 cells were seeded in 24-well plates[30], pre-mounted with glass coverslips, at a density of (1.0×10^4/well) and were allowed 24 hours of incubation time (37 °C, 5% CO2) to attach after the addition of 500 µL of both high and physiological glucose medium, followed by 0.5mM/ml and 3 mM/ml metformin treatment for 24 and 48 hrs (as described in **3.2.3.1)**. After the treatment time elapsed, the cell accommodating coverslips were washed with PBS and fixed using 4% paraformaldehyde solution[31] for 30 mins. These fixed coverslips were blocked using 20% FCS / PBS containing 0.1% Tween-20 (PBST)[32] for 1 hour, followed by overnight incubation with Anti-Glucose Transporter GLUT-1 Antibody[33] at 4 degrees Celsius (1:500 in blocking solution). The coverslips were washed 4 times with PBS the next day, incubated for 1 hour in the dark with the appropriate secondary antibodies[34] at room temperature, and then the Nuclei were stained with Hoechst 33342[35] 1:1000 (2ug/ml) for 2 mins in PBS, washed again with PBS and mounted on coverslips using Mowiol[36] and left overnight in the dark to dry. Images were acquired using Nikon A1 confocal microscope at 60X objective and analysed via ImageJ software (Fiji)[37] [54].

Image Acquisition properties: set for comparable medium intensities for both channels (Fig.15)
Hoechst (Blue channel): Laser: 2.55 – 2.8 | HV: 88 – 115 | offset: -12 to 5
Alexa 647 (Red channel): Laser: 2.9 – 3.2 I HV: 90 – 120 | offset: -10 to 5

3.6 RNA ISOLATION, REVERSE TRANSCRIPTION AND QPCR

3.6.1 RNA EXTRACTION AND REVERSE TRANSCRIPTION

Total RNA was extracted from untreated (controls) and metformin-treated SW948 Cells cultured at 1.0×10^6/well density in high and physiological glucose mediums (as described in **3.2.3.1)** using RNeasy Plus Mini kit (Qiagen)[38] according to the manufacturer's protocol [55] and then quantified by NanoDrop One[39] UV-Vis spectrophotometric analysis, A_{260}:A_{280} ratio of each sample was determined (>1.9). The total RNA from each sample was then reverse transcribed into cDNA using QuantiTect Reverse Transcription Kit[40] according to manufacturer's protocol [56] in the presence of random primers after accounting for differences in the required elution volumes on the basis of converted total amounts of RNA extracted (µg). An additional integrated removal of genomic DNA

contamination step was also performed. The Resulting cDNA samples were dissolved in RNAse free water and stored at –80 °C.

3.6.2 PRIMERS EFFICIENCY AND QPCR

Quantitative real-time polymerase chain reaction was performed in Pcr-pl 96 well plates[54] on cDNA diluted samples equivalent of 1 µg RNA using SYBR green to measure the expression of SUCLA2[41], $UCP2$[42], $PDK2$[43], $SLC2A1$[44](GLUT-1), $SLC16A3$[45](MCT4), $SLC22A1$[46](OCT1), $HSP90$[47]and $RRn18s$[48].Each reaction contained 10x Primer mix diluted in TE buffer[49], SYBR Green 2xPCR mix[50], and 10uL of cDNA. The untreated control from each culture medium served as the calibrator reference each set (HG and LG sets). Samples and calibrator were run in 2 technical duplicates obtained from a couple of distant biological samples. PCR amplification was performed using The LightCycler® 96 System[51], The PCR program was designed as follows: 95 °C preincubation for 10 min, followed by 40 cycles of 95 °C for 15 s, 55°C for 30 s, and 72 °C for 30s, finalised by one melting cycle to detect the existence of any primer dimers, further analysis was carried on using Lightcycler Software[52]. Relative copy numbers were calculated from previously calculated standard curves for each prope (efficiency > 2) and normalized to the mean expression of HSP90 and RNN using both double delta Ct method and Pfaffl to take into account the different efficiencies obtained from the standard curves of each gene.

3.7 FLOW-CYTOMETRIC ASSAYS ADDRESSING PROLIFERATION, PROTEIN EXPRESSION, AND MITOCHONDRIAL CONTENT AMID METFORMIN TREATMENT

3.7.1 SAMPLE PREPARATION.

SW948 cells were grown in 6-well culture plates (1.0×10^6 cells per well) and allowed to adhere overnight in high and physiological glucose mediums. The cells were then treated with 0.5 mM and 3 mM of metformin for 24, 48 at 37°C and 5% CO2 (as described in **3.2.3.1)**. Subsequently, the cells were dissociated enzymatically with trypsin after washing of the dead ones and pelleted by centrifugation at 900 RPM for 5 mins from each well. The resulting pallets were resuspended in PBS, centrifuged again and fixed using 4% formaldehyde in PBS for 10 minutes on Ice. After excluding 100ul of the fixed cell suspensions for cell counting and sorting purposes, they were divided into 2 equal aliquots,

one set was stored 4°C to investigate cell surface markers, while the second set was Permeabilized in 90% methanol on ice after removing the centrifuged PFA supernatant and stored at -20 to be used for assessing mitochondrial content.

3.7.2 FLOW CYTOMETRIC PROLIFERATION ASSESSMENTS AND CELL SORTING.

In order to further establish metformin effects on SW948 cell growth and to selectively obtain a more desirable population for GLUT-1[33] and Tomm20[53] analysis to come, an initial flow cytometry assay took place using the reserved 100ul cell suspensions. Flow cytometric cell sorting and analysis were performed using Accuri c6 flow cytometer[54], and was used to aliquot equal number of cells in all specimen tubes for following experiments.

For each sample, the cell suspension was washed twice to remove traces of PFA, diluted in 250ul of PBS and then was aspirated fully into the instrument.

3.7.3 ESTIMATION OF MITOCHONDRIAL CONTENT USING FLOW CYTOMETER.

Fixed samples were centrifuged and resuspended in incubation buffer to wash off PFA remains two times before starting the Primary antibody labelling with TOM22 in incubation buffer away from light for 1 h at room temperature. Samples were run through Accuri C6 flow cytometer after being washed and finally resuspended in 500 ml of PBS.

3.7.4 FLOW CYTOMETRIC ANALYSIS OF GLUT-1 EXPRESSION

90% methanol permeabilized and fixed samples were used to assess GLUT-1 expression. After washing in PBS, and repeatedly resuspended in Incubation buffer (3 times), the samples were incubated with glut-1 primary antibody (1:500 in 100 uL incubation buffer) for 1 hour at room temperature. 2 extra washes were performed before labelling the cells with secondary antibodies for 30 minutes in the dark at room temperature. The stained cells were washed again and resuspended in 500 ml PBS and then analysed using Accuri C6 flow cytometer.

3.7.5 DATA ANALYSIS:

Further analysis was carried on using FlowJo[55] to isolate homogeneous populations of single cells that makes most of the studied sample and compare it to populations undergoing mitoses and doublets of cells (Fig.5).

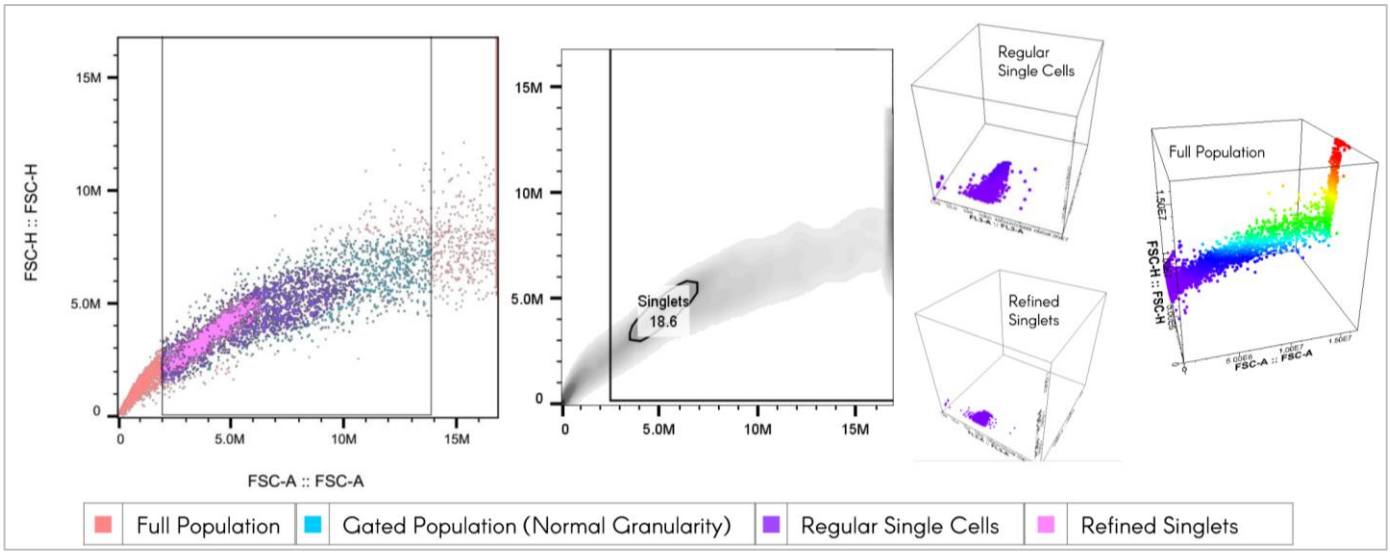

FIGURE 5 *flowcytometry gating and cell sorting processes*

To the left A dot-scatter 3-step isolation process starting with the debris dismissal (in lines) followed by identifying a conformed side-scatter of the cells (in cyan) and then isolating 2 populations of interest to further analysis. Further demonstrations of various populations are shown grey cycle density scatter and 3d scatters.

3.8 STATISTICAL ANALYSIS

Statistical analysis of data was carried on using independent student t-test for equal or unequal variances depending on the F-value for a given test. Analysis of variance (ANOVA) were done when appropriate using excels analysis ToolPak – VBA.

CHAPTER 4. RESULTS

4.1 PHYSIOLOGICAL GLUCOSE CONDITIONS PROLONGS THE DOUBLING TIME OF THE HIGHLY GLYCOLYTIC SW948 COLORECTAL CANCER CELL LINE

To further understand the growth variance under physiological glucose and high conditions which favour proliferation, the doubling time was calculated in SW948 Cells cultured in 1g/L glucose versus 4.5g/L. The growth was proceeding at a notably elevated rate when grown in high glucose (Fig.6 A) presenting 6.52-fold increase after 72 hours compared to cells cultured in physiological glucose (Fig.6 B) which grown to a maximum of 3.2 times more when allowed the same time. The difference in growth rate showed a linear progression over time with a slope of 0.05 (Fig.7 B) and the calculated doubling times using exponential growth demonstrated that increase as the doubling time was significantly faster in high glucose 25.2 hrs versus 39.8 hrs in physiological glucose (Fig.7A).

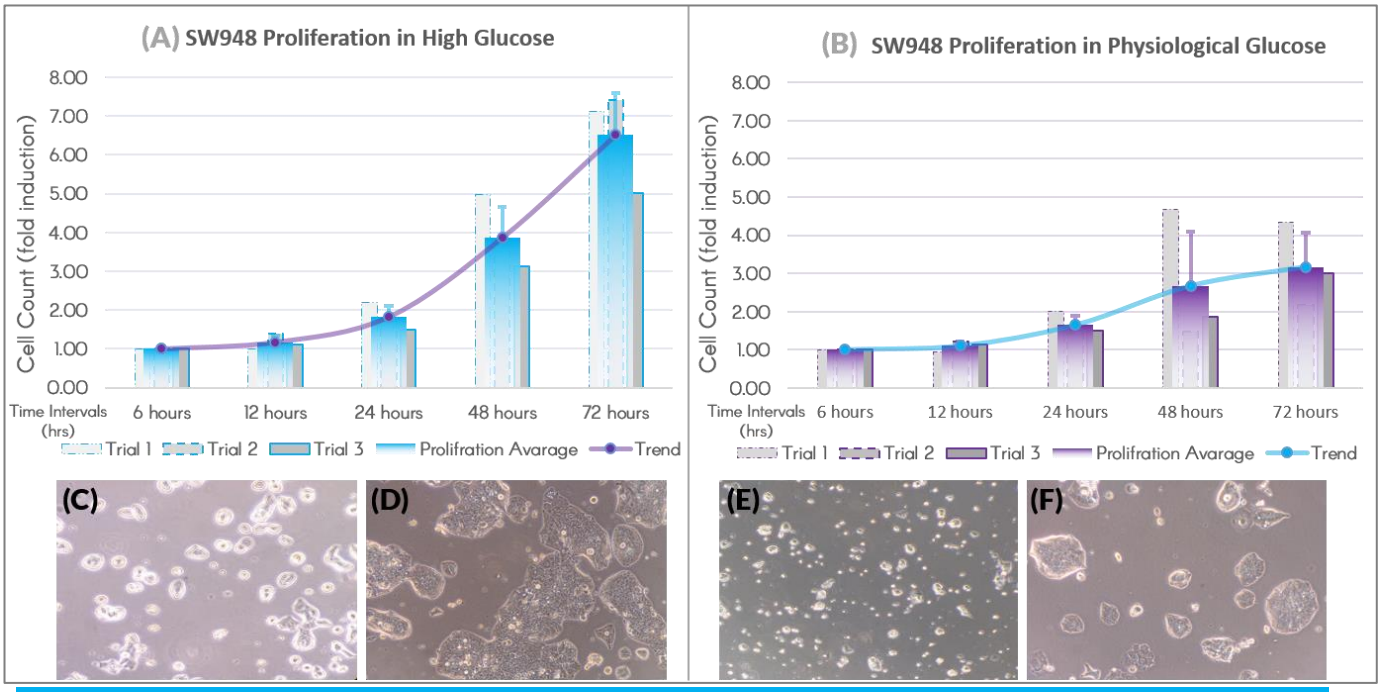

FIGURE 6 *Different SW948 Proliferation rates over 72 hours in high and physiological glucose media.*

(A): Proliferation rate average from 3 biological triplicates cultured in High glucose versus physiological glucose (B). Images of cell cultures demonstrating the difference were taken by light microscopy after 12 (C) and 72 (D) hours in HG and in LG (E) and (F) respectively. StDev for HG are 0.16, 0.28, 0.8, 1.07 and for LG are 0.12, 0.25, 1.42, 0.89 corresponding to 12, 24, 48, 72 hours intervals accordingly.

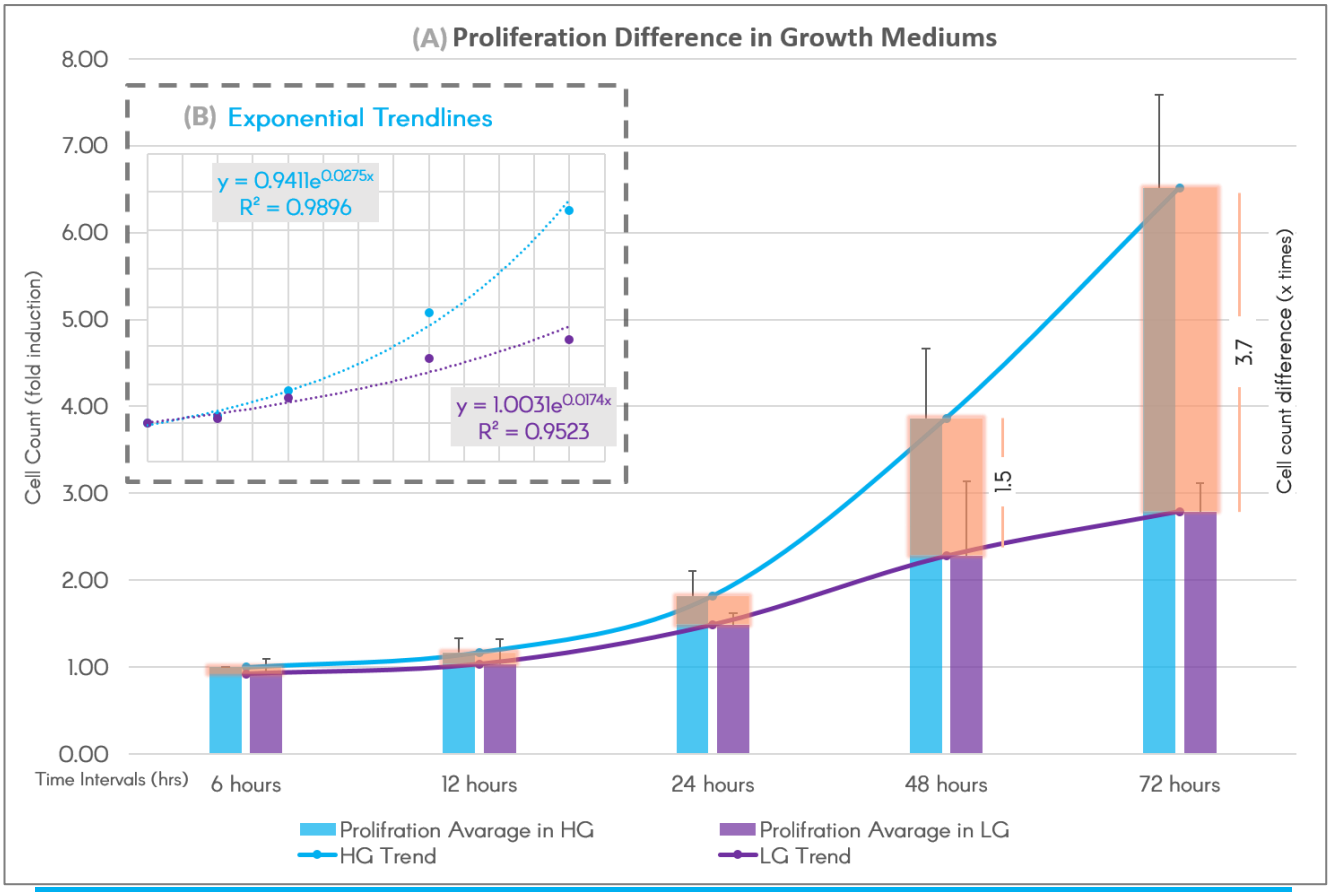

FIGURE 7 *Comparison of the Differential growth rates in HG and LG culture media.*

(A) growth trends plotted side by side to show the difference in proliferation, achieving 1.5, 3.7 more induction after 48, 72 hrs in high glucose than physiological glucose (t= 5.8, 3.4) (P= 0.009, 0.04) respectively. **(B)** exponential curves and derived function equations used to calculate growth rates 0.0275, 0.0174 for HG and LG trends respectively.

4.2 METFORMIN INHIBITS SW948 PROLIFERATION DIFFERENTLY UNDER HIGH AND PHYSIOLOGICAL GLUCOSE

To question the inhibiting actions of Metformin on the proliferation of glycolytic CRCs, SW948 cells were maintained in physiological and high glucose conditions for 72 hours and subjected to a series of Metformin treatments, 0.1mM, 0.5mM. 1mM, 3mM & 5mM over 48 hours. The optical density (OD) of each well was measured at 492 nm after 4 h MTS incubation using Thermofisher Muktiskan ascent plate reader after an added 30 seconds of shake time. The triplicate of untreated cells was used as the control, and the blank wells were used to subtract background readings. The following formula was used for calculating cell viability of the averaged triplicate reading:

$$Cell\ Viability\ (\%) = \frac{OD_{492}(Sample) - OD_{492}(Blank)}{OD_{492}(Control) - OD_{492}(Blank)} \times 100$$

where OD = optical density

After the first 24 metformin exposure in high glucose, lower concentrations of metformin appear to result in lesser viable cells (0.1mM and 0.5mM; 15% less viability with low significance P=0.25, 0.14 respectively) while higher metformin concentrations showed reduced effectiveness (1mM, 3mM and 5mM; 8-12% less viability also with negligible significance P=0.28, 0.71, 0.55) (Fig.8). The cells followed an initial dose-dependent trend after 48 hours registering a viability of 21% less using 1mM of metformin (t=5.7 P=0.00013).

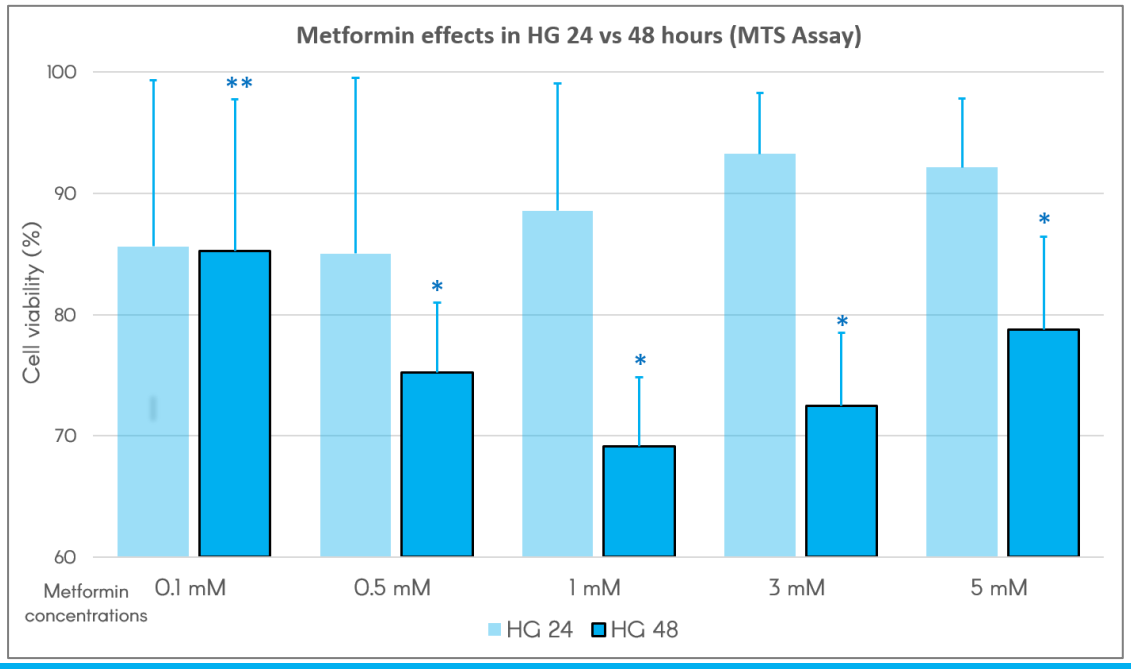

FIGURE 8 *Comparison of Metformin anti-proliferative effects in HG in 24hrs vs 48hrs.*

A series of 0.1 mM, 0.5 mM, 1 mM, 3 mM and 5 mM of metformin concentrations resulted in the viability percentages after 24hrs: 85.61%, 85.04%, 88.58%, 93.27%, 92.14% after 48 hours of 85.25%, 75.22%, 69.14%, 72.49%, 78.74 respectively. (* T-test, P<0.05) (** T-test, P<0.01)

Under physiological glucose conditions, MTS results after 24hrs kept showing plumbing viability with escalating doses of metformin registering its lowest viability (18% less) with 3mM (P=0.12) of metformin, while 5mM failed to match the same levels with 13% decline in viability (P=0.3). In the subsequent reading at 48 hours, SW948 cells responded in a similar pattern and were affected further with the longer time exposure with 21% less viability at 3mM (T=4.4, P=0.0004) (Fig.9).

Measurements after 48 hours were more consistent and showed that metformin in physiological glucose would be most effective at 3mM concentration while 1mM was the most effective in high glucose showing similar viability reduction (Fig.10).

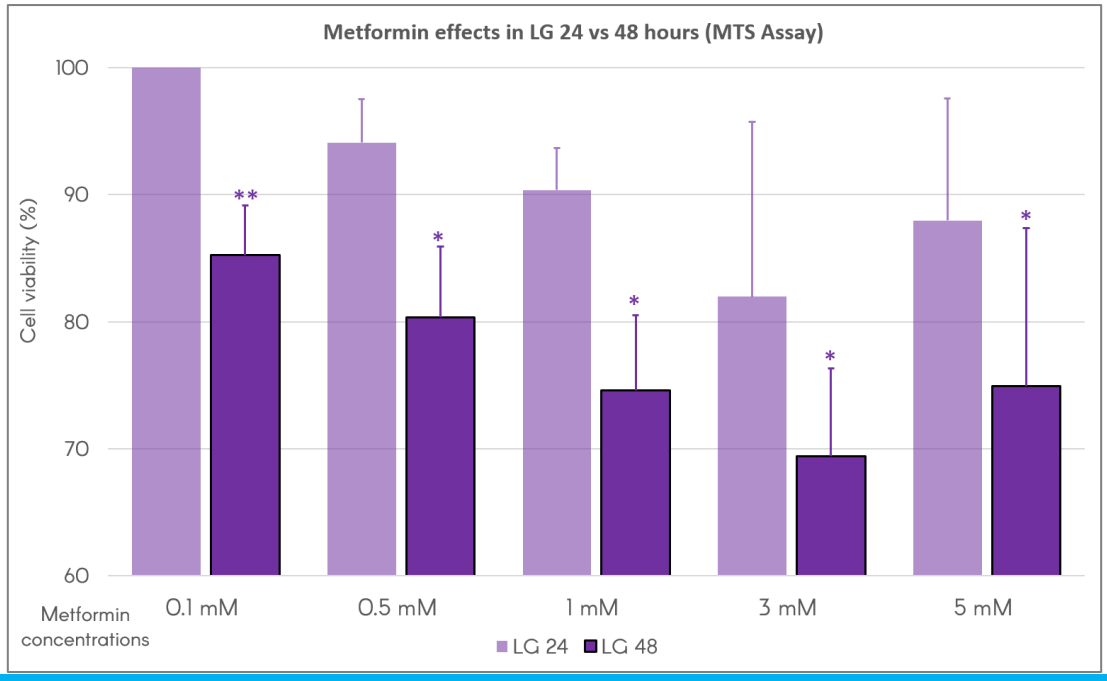

FIGURE 9 *Comparison of Metformin anti-proliferative effects in LG in 24hrs vs 48hrs*

A series of 0.1 mM, 0.5 mM, 1 mM, 3 mM and 5 mM of metformin concentrations resulted in the viability percentages after 24hrs: 101.03%, 94.12%, 90.37%, 81.97%, 87.98% and after 48 hours of 85.24%, 80.33%, 74.62%, 69.41%, 74.95% respectively. (* T-test, P<0.05) (** T-test, P<0.01)

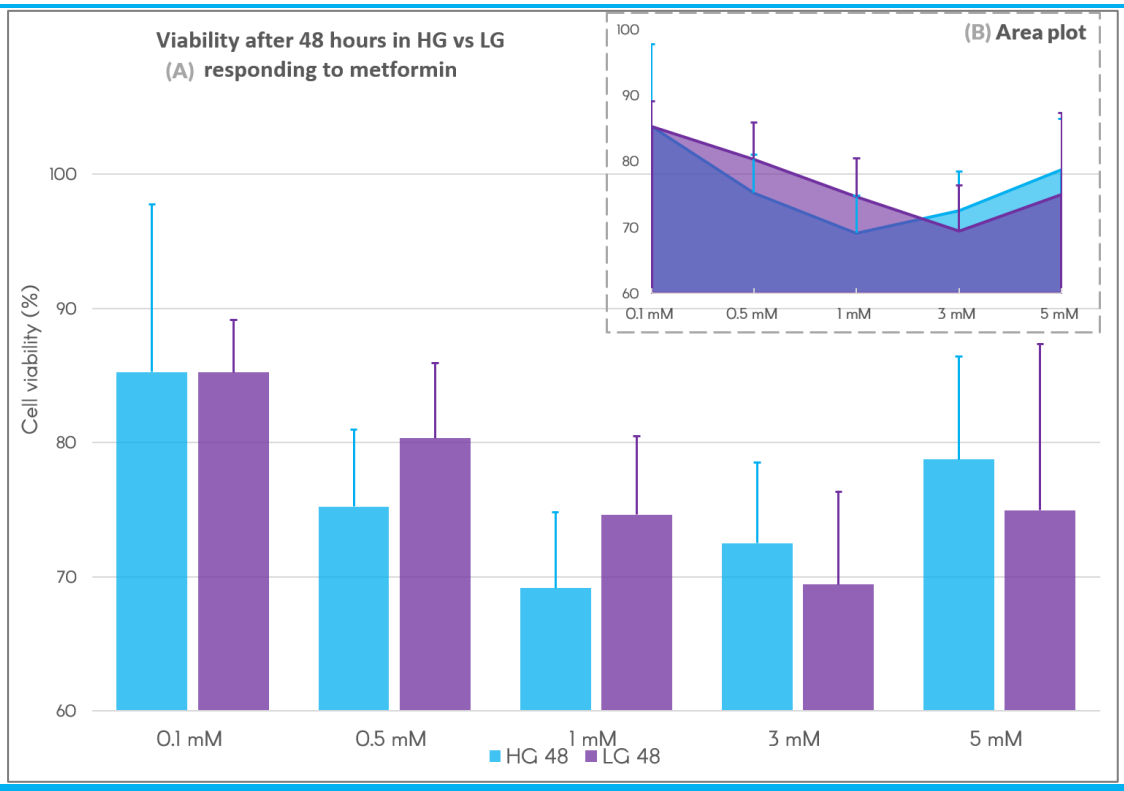

FIGURE 10 *Metformin effects on viability after 48 hours in High (HG) and Physiological Glucose (LG)*

(A) Comparative MTS results of metformin effects for the tested serial concentrations after 48 hrs. **(B)** An area plot of the same diagram that better illustrate the peak effects of metformin in each culture media, high glucose being shown in cyan, compared to physiological glucose in purple.

4.3 PHYSIOLOGICAL GLUCOSE CONCENTRATIONS ENFORCE HIGHER GLUT-1 EXPRESSION FURTHER INCREASED WITH METFORMIN, WHILE DOWNREGULATED WHEN CULTURED IN HIGH GLUCOSE CONCENTRATIONS

To test SW948 cell line metabolic response in terms of glucose uptake after metformin treatment in high and physiological glucose media, a measurement of GLUT-1 protein in prepared lysates by Western blot analysis took place after an initial total protein assessment using BCA. The intensities of the bands observed between 38-55kDa were further analysed with Bio-Rad Image Lab Software to define the exact outlines using lane profiles. Metformin attributed in a slight gradual decrease of GLUT-1 when treated in high glucose conditions. The same was observed after 24 hours in physiological glucose, but extended exposure (48 hours) displayed an elevated dose-dependent expression of GLUT-1, notably present at 3mM doses of metformin (Fig.12). Exposure to physiological glucose concentrations doubled GLUT-1 expression and further elevated with 3mM metformin treatment after 48 hours at 2.3-fold increase (n=4 individual experiments) (Fig.11, Fig.12).

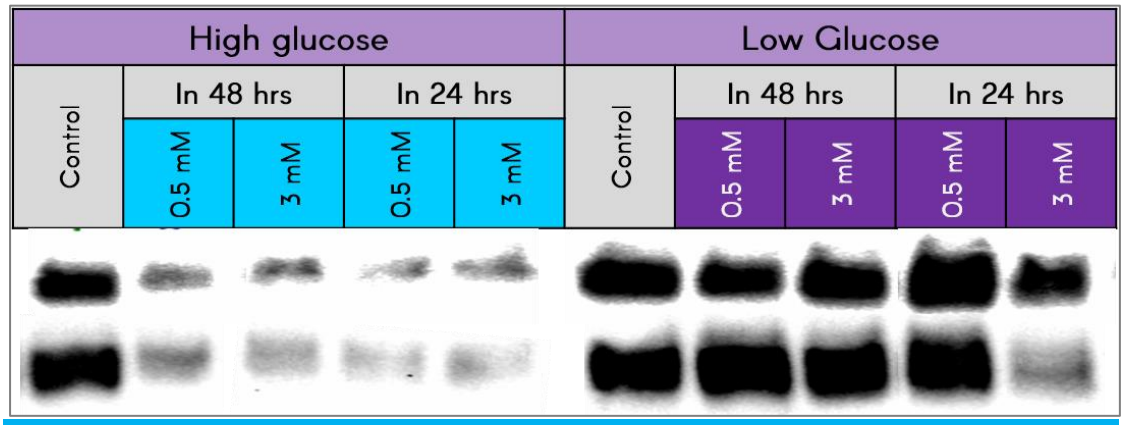

FIGURE 11 *Western blot of Glut-1 expression in HG and LG in response to metformin.*

Membrane examples that are used to estimate Glut 1 expression, Normalization was done according to stain free total protein lane normalization.

All lanes: Anti-GLUT1 AB: 1/100,000

Secondary AB: Goat Anti-Rabbit IgG H&L (HRP) 1/100,000

Dilution buffer: 3%NFDM/TBST – **Blocking buffer**: 5% NFDM/TBST

Predicted band Size: 54kDa – Observed Band Size: 38-55kDa – Exposure time: 50 seconds

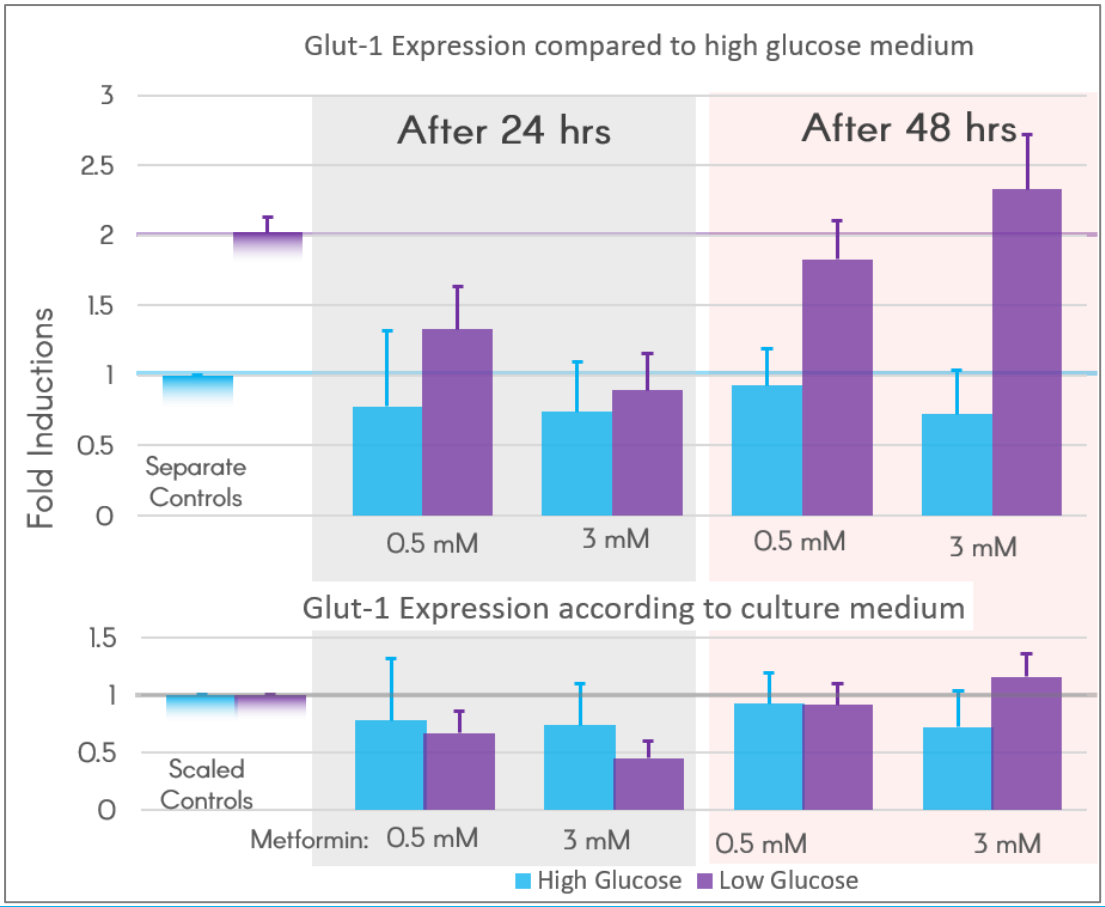

FIGURE 12 *Western-blot Glut-1 expression in response to metformin treatment.*

Top bars demonstrate glut-1 expression variances in response to metformin in all samples compared to high glucose (control). Bars below indicate glut-1 expression in both sets after metformin treatment each compared to an equally scaled control (=1). Results are obtained from analysed band intensities of western plots shown in (Fig.11)

4.4 METFORMIN REDUCE THE SURFACE EXPRESSION OF GLUT-1 IN NON-PERMEABILIZED SW948 CELLS

To assess the colocalization and further establish the expression levels of Glut-1 in metformin-treated SW948 cells cultured in high and physiological glucose. Confocal stack images of immunofluorescence-stained cells were further analysed using ImageJ according to a standardized relative quantification protocol [57]. Briefly, 5 distinct frames were captured as stacks from every specimen, with integrated density (IDV) being the main measurement meter. The average nuclei integrated density was calculated separately for each specimen by measuring the average of 10 distinct ROI outlined nuclei IDVs. The average nuclei integrated density was then used to calculate the number of cells per frame (Total hoechst IDV/average nuclei integrated density) and eventually quantify the average GLUT-1 expression per cell (Total GLUT-1 IDV/number of cells). Median GLUT-1 expression levels show a significant elevation (1.8 folds) in physiological control samples when compared to high glucose control (Fig.13) consistent with that seen in the western blot analysis (section 3.3.3). A higher EMT morphology incidence (Fig.15) was observed in physiological control, which could attribute to the higher glut-1 expression quantified. Even though the previously mentioned elevation was seen across all physiological glucose samples when compared to their high glucose counterparts, the addition of metformin seems to cause a dose-dependent reduction in cell surface GLUT-1 levels detected in fixed (non-permeabilized) SW948 cells. However, this reduction was repelled with extended exposure time to metformin, peaking at 1.42-fold increase using 0.5 mM metformin for 48 hours (Fig.13). Overall, confocal stack images of 2 distinct biological GLUT-1 Stained samples were analysed, generating 173 data points accounting for 7903 cellular measurements. The data points were further box plotted (Fig.14) indicating similar trend.

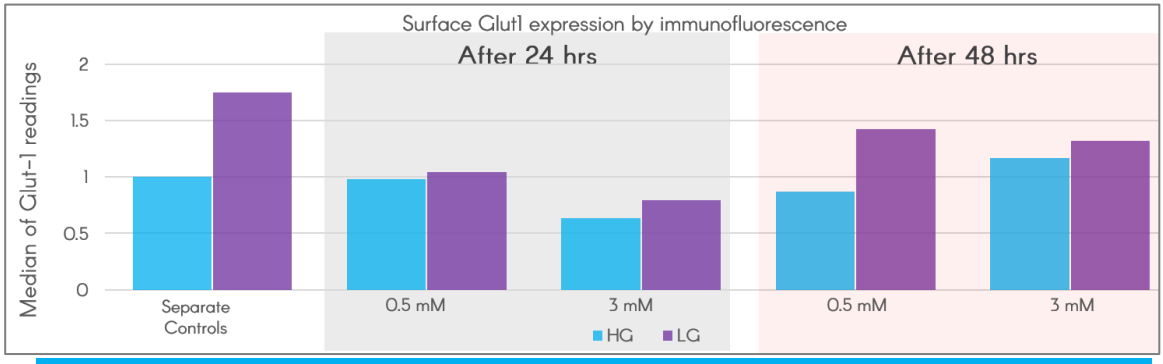

FIGURE 13 *Glut-1 surface expression obtained by confocal imaging*

Median GLUT-1 expression fold inductions obtained from confocal imaging frames analysis in both culture media responding to 0.5mM and 3mM metformin treatment.

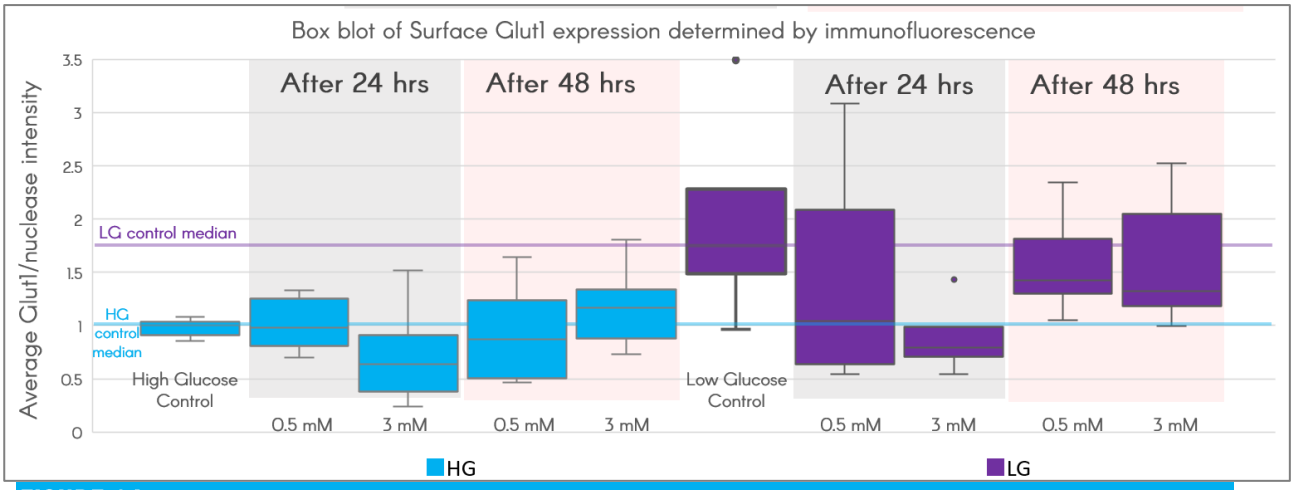

FIGURE 14 *Boxplot representation of Metformin effects on the expression of surface GLUT-1*

Calculated GLUT-1 to nucleus averages represented in boxplot. The comparison mainly shows a higher surface glut-1 expression for cells cultured in physiological glucose than high glucose medium.

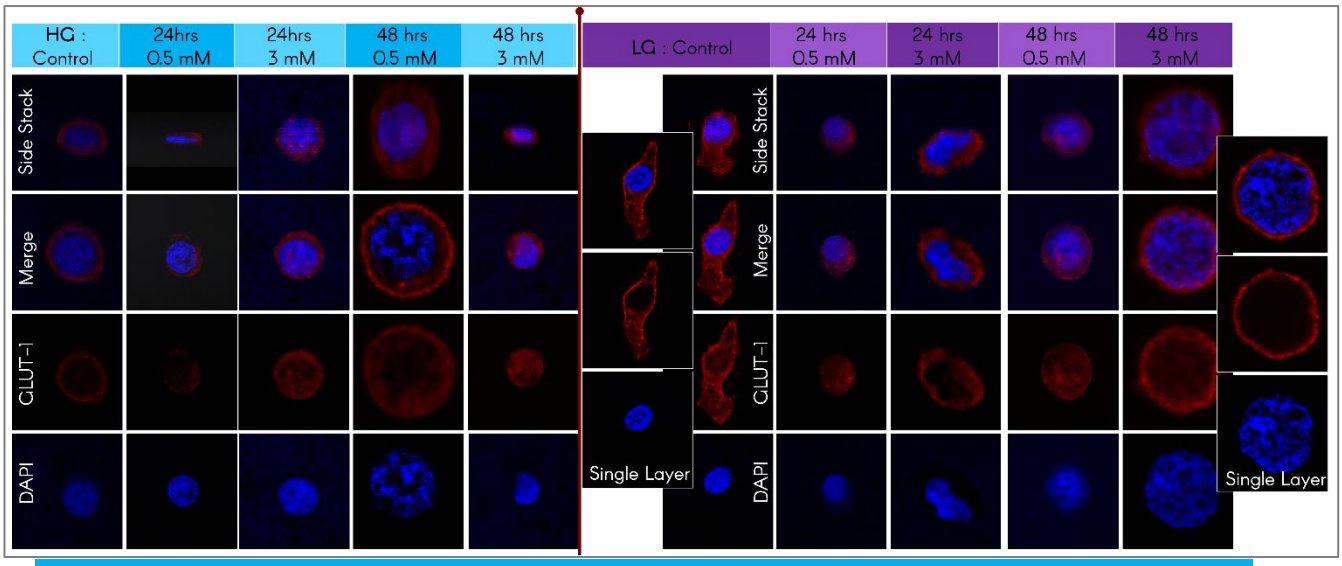

FIGURE 15 *Confocal imaging examples of glut-1 expression immunofluorescence*

Examples of SW948 cells confocal images in both culture HG and LG media amid 0.5mM and 3mM metformin treatment. the shown image lanes from top to bottom represent the Z-stack in a depth view (sidestack), maximum intensity projection of the Z-stack for both Far Red (glut-1) and DAPI (Hoechst/nucleus), separate Far Red channel (Alexa 647), separate DAPI channel. The single layer images (triplets) are selected singular frame from the Z-stack to show the observed EMT in LG Control and Glut-1 expression in 3mM treatment after 48 hours.

For all slides: Glut-1 AB: 1/500 – secondary AB: 1/1000 – Hoechst (2ug/ml): 1/1000

4.5 GENE EXPRESSION ANALYSIS

To extend the understanding of the effects metformin have on SW948 cells, expression levels of key genes involved in energy metabolism and metformin uptake has been examined. After establishing the efficiency of the used primers (>1.8 results in the appendix), the estimated Cq values showed 4 genes with consistent regulation trends in response to metformin and different glucose conditions.

4.5.1 GLUT-1 MRNA LEVELS REGULATED INVERSELY IN HIGH AND PHYSIOLOGICAL GLUCOSE CONDITIONS

The mRNA expression of GLUT-1 obtained from high glucose cultures increase slightly 1.1~1.3 and 1.8~6 folds increase while treating with 0.5 metformin for 24 and 48 hours respectively. While 3mM doses seem to downregulate GLUT-1 levels dose-dependently on an average of 0.5 and 0.35-fold of control (Fig.16).

On the other hand, physiological glucose conditions showed a clear upregulation compared to high glucose, close to 2 folds increase, which matches the GLUT-1 protein expression observed with western blotting. The addition of metformin seems to quickly upregulate GLUT-1 expression dose dependently after 24 hours with 1.85 and 3.44 fold increase for 0.5mM and 3mM respectively, while the expression rate seems to downregulate after 48 hours with 0.5mM, it stays upregulated using 3mM metformin between 2.85 to 4 fold increase (Fig.16).

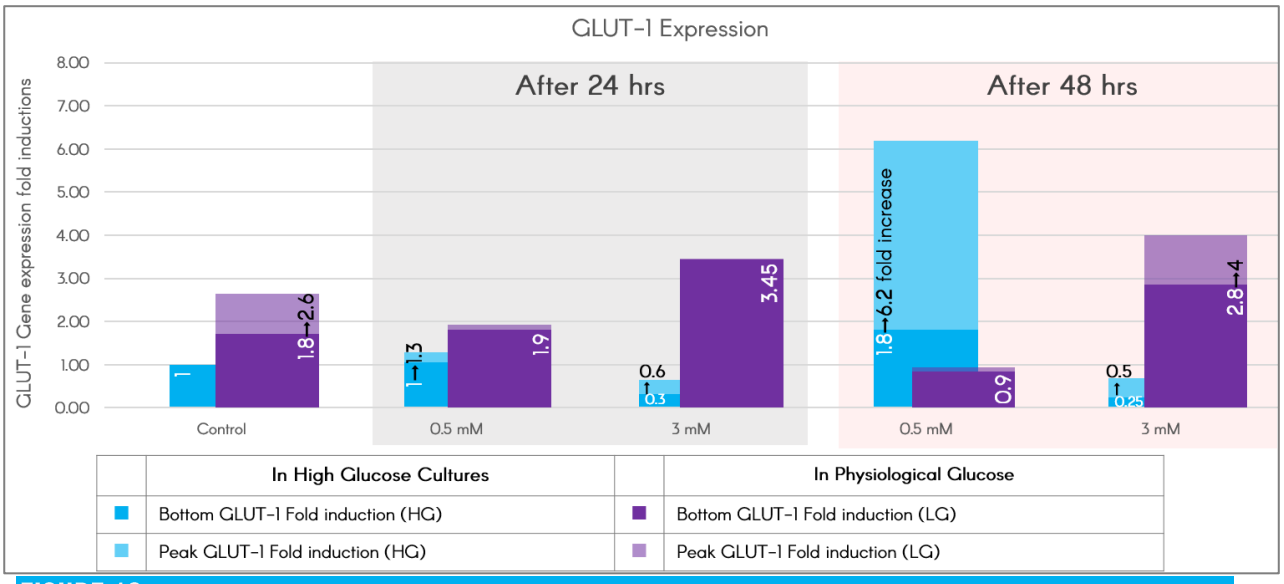

FIGURE 16 *GLUT-1 Gene expression in response to metformin treatment*

Stacked bar representation of GLUT-1 gene expression fold inductions in 24 and 48 hours responding to 0.5mM and 3mM of metformin treatment.

4.5.2 SW948 RESPONDS TO METFORMIN TREATMENT BY REDUCING OCT-1 EXPRESSION

Examination of OCT-1 mRNA levels, which is responsible for the uptake of metformin into the cell, revealed that it is downregulated in exposure to metformin dose-dependently regardless of glucose levels, showing 0.6~0.9 fold reduction variance. Yet, extended exposure seems to modulate OCT-1 back close to average using 0.5mM metformin, and downregulates it even further using higher doses (3mM) (Fig.19).

4.5.3 ELEVATED UCP2 AND PDK2 EXPRESSION IN PHYSIOLOGICAL GLUCOSE IS ANTAGONIZED BY HIGHER CONCENTRATIONS OF METFORMIN

The impact of metformin on energy regulation of SW948 was evaluated by investigating the mRNA levels of PDK2 and UCP2. The former encodes a protein that phosphorylates pyruvate dehydrogenase, while the latter is part of the mitochondrial uncoupling proteins family and responsible for proton leak. UCP2 expression increased in a positive correlation with metformin concentrations in high glucose samples to a maximum of 9.5-folds. While physiological glucose levels appear to generally impose higher expression rates (2~26-folds more than high glucose), increasing doses of metformin decreased UCP2 mRNA levels in 48 hours samples (Fig.17).

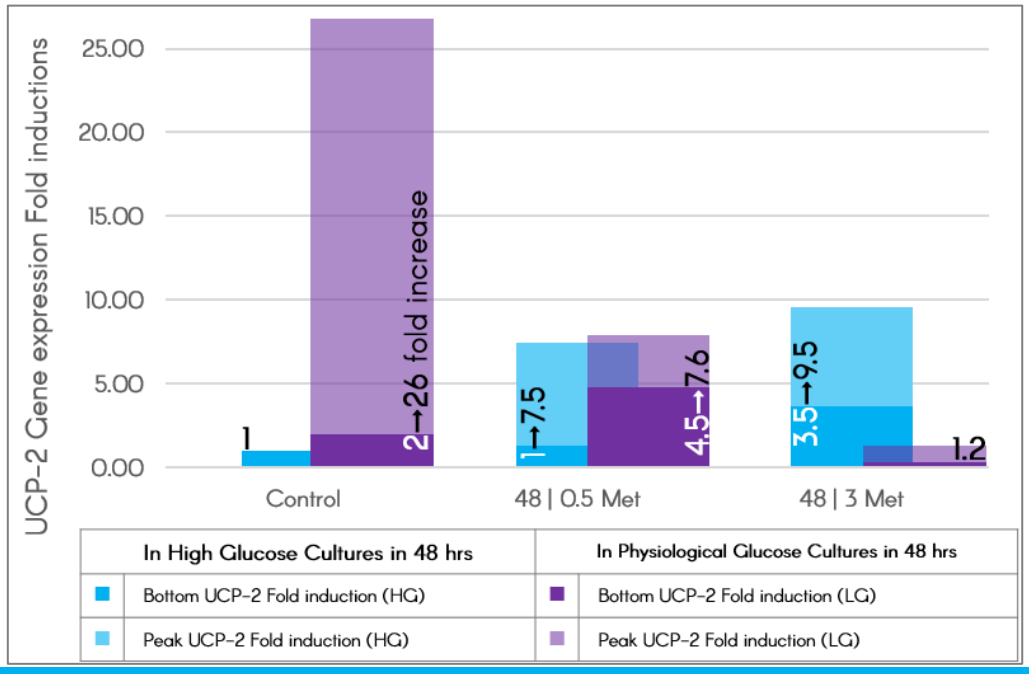

FIGURE 17 *UCP-2 Gene expression in response to metformin treatment*

Stacked bar representation of UCP-2 gene expression fold inductions after 48 hours of 0.5mM and 3mM of metformin treatment.

Though slighter changes have been observed in PDK2 mRNA levels, quite a similar trend can be seen physiological glucose cultures. The upregulated PDK2 in physiological glucose seems to decline dose dependently with increasing concentrations of metformin (0.8~1.2-fold of control in 3mM metformin treatments), in comparison to an almost plateau reaction in high glucose condition (Fig.18).

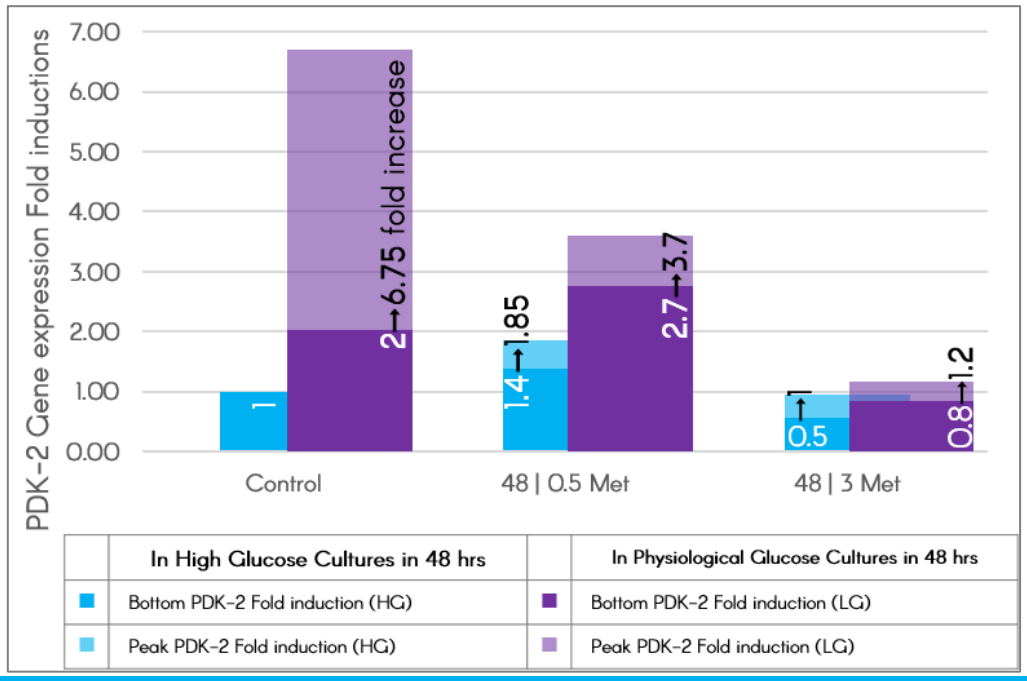

FIGURE 18 *PDK-2 Gene expression in response to metformin treatment*

Stacked bar representation of gene expression fold induction of PDK-2 after 48 hours of 0.5mM and 3mM of metformin treatment.

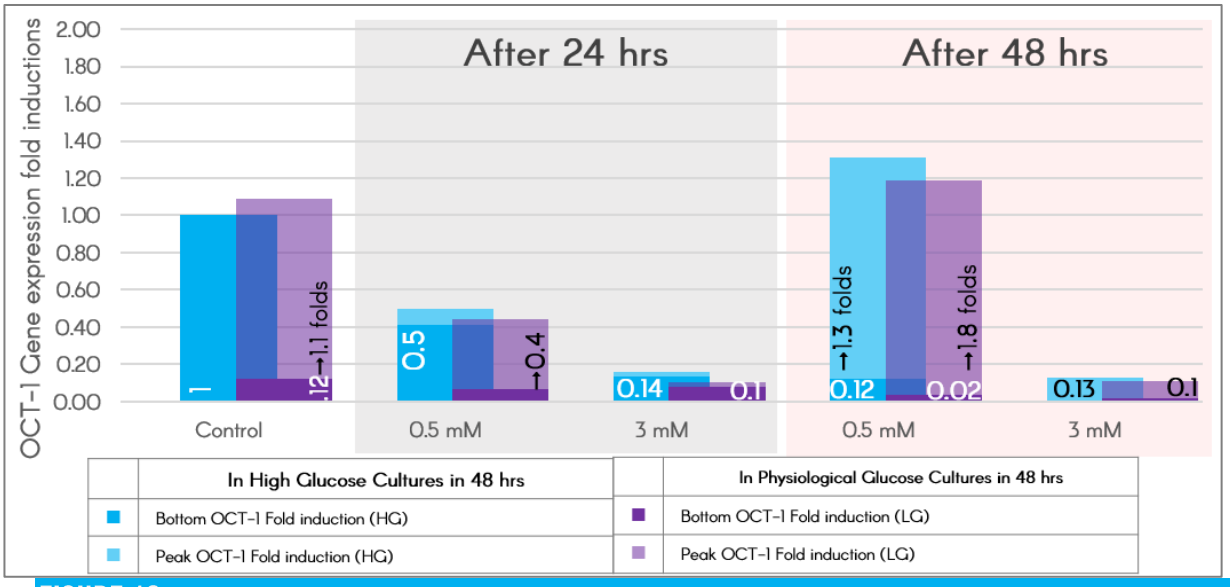

FIGURE 19 *OCT-1 Gene expression in response to metformin treatment*

Stacked bar representation of OCT-1 gene expression fold inductions in 24 and 48 hours responding to 0.5mM and 3mM of metformin treatment.

4.6 FLOW-CYTOMETRIC ANALYSIS

4.6.1 FLOW CYTOMETRIC ASSAY CONFIRMED THE RESTRAINING EFFECT OF METFORMIN ON PROLIFERATION

A constant volume of 100uL was used to measure the differences in cell numbers after seeding equal densities via flow cytometry. The results confirmed the effects of metformin inhibiting proliferation (MTS results in section 4.2) descending steadily with increased concentrations and exposure time in high glucose medium to 77%, 60%, 38% and 30% of control in 24 hours using 0.5 mM metformin, 3 mM metformin, 48 hours using 0.5 mM metformin and 3 mM metformin respectively (Fig 20). The effects of physiological medium were observed with a drop to 64% compared to high glucose control, and while there was no significant change in numbers in 24 hour treatments, they dropped dramatically after 48 hours exposure to metformin to 33% and 18% in 0.5 mM and 3mM treatments respectively (Fig.20).

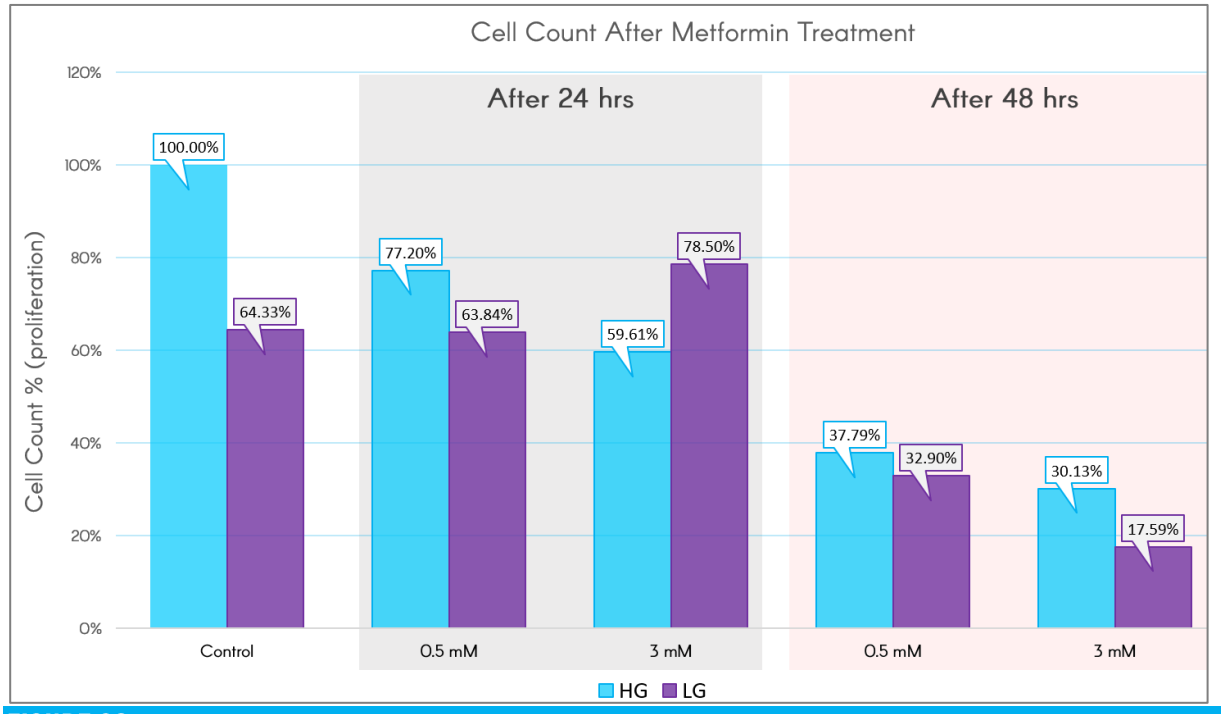

FIGURE 20 *Proliferation Rate correlated with flowcytometric cell count events*

Proliferation rates of SW948 cells after metformin treatment in both culture media correlated to the number of gated events in 100uL of aspirated homogenous cell solution.

4.6.2 CELL SIZE AND ACCUMULATION AFFECTS THE ESTIMATION OF GLUT-1

GLUT-1 protein expression levels were examined in a different way using flow cytometry individualizing homogeneous single cells and a larger debris free populations containing larger sizes and cells undergoing mitosis. The larger population showed an increased GLUT-1 expression attributed mainly to physiological glucose conditions (1.7-fold increase) elevating in response to metformin exposure (1.92-fold increase in 48 hours 3mM metformin concentrations) a seen in western blot analysis (section 4.3) (Fig.21 A). On the other hand, whereas glucose concentrations still play the major rule in GLUT-1 expression in homogeneous single cells subpopulation (1.72 fold increase), it appears to be the protein levels are going downwards in response to higher metformin doses (1.62-folds in 3mM metformin treatment after 48 hours) in a pattern similar to the one observed with confocal imaging (section 4.4 Fig.15) (Fig.21 B).

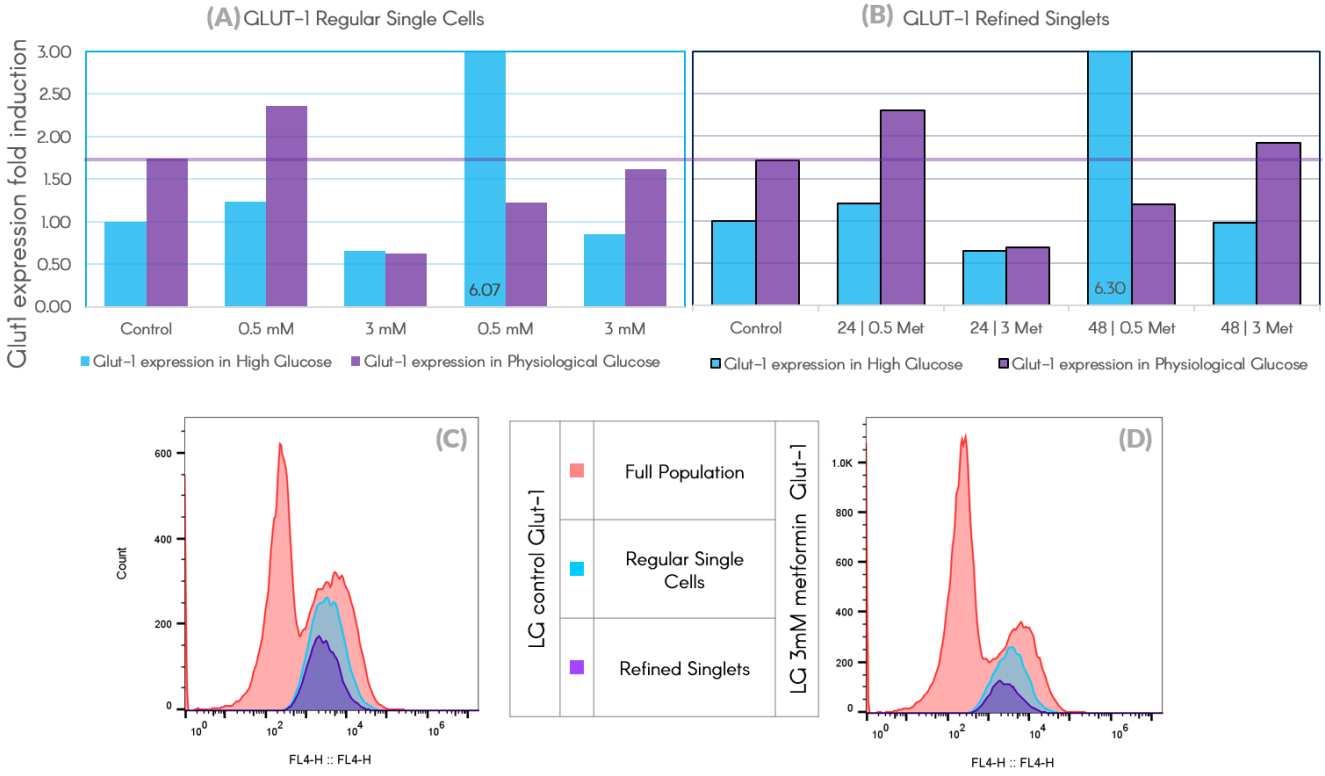

FIGURE 21 *Flowcytometric assessment of Glut-1 expression after metformin treatment*

(A) detected fluorescence correlated to expression rates of surface GLUT-1 after metformin treatment in both mediums of gated events in contrast to **(B)** refined singlets. At the bottom height fluorescence histogram for both populations of interest in displaying LG control **(C)** and 3mM metformin treatment after 48 hours **(D).** 48hrs treatment of 0.5 mM Metformin in HG displayed inaccurate measurements, and therefore disregarded, due to excess of Glut-1 AB rendering it unreliable.

4.6.3 METFORMIN INDUCED AN INCREASE IN MITOCHONDRIAL CONTENT IN HIGH AND PHYSIOLOGICAL GLUCOSE CONDITIONS

Alterations to mitochondrial content of SW948 cells in response to Metformin was assessed via their expression to TOMM20, a mitochondrial outer membrane protein that in non-permeabilized cells correlates with functional mitochondrial mass. Flowcytometric assay revealed that metformin invariably induced a gain in mitochondrial content up to 1.7 times more than control. However, physiological glucose conditions alone had a very slight impact but modulated a constant time-dependent mitochondrial mass elevation in response 0.5mM concentrations of Metformin, 1.22 and 1.56 fold increases after 24 hours & 48 hours respectively. 3mM concentration had an even effect of 1.6 fold increase over both times intervals. The observed mitochondrial content in high glucose conditions complied to the time-dependent increasing pattern in 0.5mM of metformin treatment, 1.37 and 1.47 fold increases after 24 hours & 48 hours accordingly, while showed a decline overtime using 3mM metformin from a peak of 1.71 in 24 hours to 1.26 fold inductions after 48 hours (Fig.22).

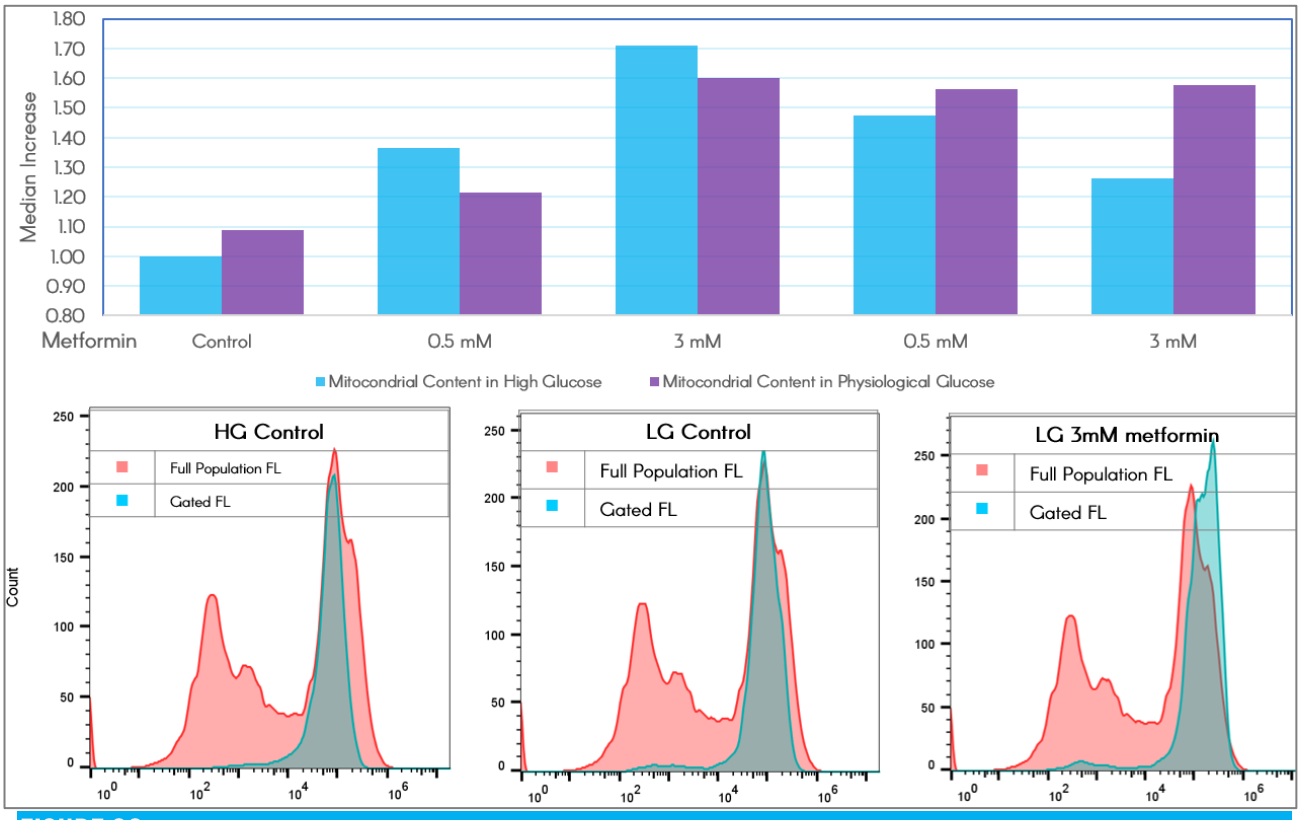

FIGURE 22 *Flowcytometric assessment of mitochondrial content after metformin treatment*

At the top is the median of the detected TOMM20 fluorescence correlated to the mitochondrial content after metformin treatment in both mediums of gated events. At are selected height fluorescence histograms for HG control, LG control, 3mM metformin treatment in low glucose illustrating gated population (in cyan) overlaying full population (in red).

CHAPTER 5. DISCUSSION

5.1 DISCUSSION OF RESULTS

The previously observed glycolytic phenotype of the SW948 cell line is in itself an indicator of a heightened proliferation and possibly invasiveness. While *in-vitro* observations confirm a remarkably high proliferation rate, the full proliferative capacity is best attained in the abundance of glucose as expected. This excess of glucose could be a driving factor for the metabolic shift from oxidative phosphorylation to glycolysis in cancer cells granting them the invasive and rapid growth criteria [4]. The use of physiological glucose medium to culture the SW948 cell is thought to predict a proliferation trend more comparable to what might occur *in vivo*. The results showing a big difference between the trends (Fig.7) are an indicator of variant activation levels of metabolic pathways involved in tumour growth, especially PI3K pathway considering its ability to localize GLUT1 at the plasma membrane. however, this needs to be confirmed with further analysis of proteins involved in this pathway. Considering the caliber of glucose levels effect on cellular metabolism is vital to the assessment of Metformin effects in the cells as it could influence the degree of its capabilities. The notably similar growth pattern observed in the first 24 hours using both culture media (Fig 5,6,7) could be explained as a post-trypsinization lag time (represented in one cell cycle) before the cell is able to optimize its metabolic pathways for maximum growth in regard to its microenvironment. This is clearly seen in the HG set's exponential growth after 48 and 72 hours, opposed to a slightly elevated growth trend in LG preserving their tumour proliferative capabilities in physiological glucose but at much lesser rate due to a moderate alteration of metabolic pathways (Fig.7).

The addition of serial concentrations of metformin to both previously mentioned media sets uncovered different corresponding effective doses. In a general look, comparing the effects at both time intervals (24, 48hrs), it seems that metformin requires some time before starting to reflect consistent outcomes in a dose dependant and an exposure dependant manner (Fig.8,9). The observed dose dependency varied across cells cultured in HG and LG media. Cells cultured in HG seems to sensitize at a lower concentration of metformin (1mM) followed by resilience against higher concentrations, while cells cultured in LG needed (3mM) to mimic a proportional outcome. To explain this, a couple of factors need to be considered. First, MTS assay's correlation with viability is derived from the NADPH mediated formation of the measured coloured formazan [58]. As NADPH is either

generated through PPP or mitochondrial metabolism, the former is very dependent on glucose availability, while the latter is dependent on the mitochondrial functionality as seen in cancer cells experiencing glucose limitation, making the TCA-intermediates-dependant mitochondrial fatty acid oxidation from malate and citrate the major source for NAPDH [16,59]. The second point revolves around AMPK-mediated NAPDH regulation. When activated, AMPK maintains NADPH levels by a ACC1/2-mediated coordination of fatty-acid metabolism, which inhibits synthesis (FAS) and promotes its oxidation (FAO). While metformin is known to activate AMPK, it is important to note that glucose deprivation is a major prompter to its activation as well [59]. Thus, in certain cases, the redox regulating effects of modestly high amounts of metformin could theoretically prolong cell survival through the AMPK mediated NADPH regulation [59]. To apply this in the HG/LG media sets scenario used in this research, it could be argued that the AMPK-independent metformin effects are the main drivers of cell death (or maybe apoptosis) at tested concentrations. The need for higher doses of metformin in LG could be reasoned to the fact that culturing at low glucose levels itself triggers AMPK. Therefore, higher concentrations of metformin are needed to establish AMPK-independent actions able to overcome the AMPK mediated NADPH compensation. Nonetheless, increasing metformin concentrations to 5mM seems to revert the cells back to a better viability status in the absence of a chemotherapeutic agent, suggesting the existence of a dosage window where lowest viability rates could be achieved using metformin alone (between 1mM and 3mM of metformin). It is important to stress that the previous reasoning is solely based on MTS assay results and its tight connection with NAPH levels, the phenomena observed here may or may not occur using other tests and therefore further research is required to establish it. In light of these results, and a further confirmation of metformin dose-dependent anti-proliferative effects using flow cytometry after 48 hours exposure (Fig.20), 3mM was selected for further testing as it seems to best replicate the physiological condition.

To assess metformin's underlying mechanisms on SW948 cell-line, an arguably rate limiting transporter for glucose metabolism, GLUT-1 [4, 60] was further considered due to its involvement in maintaining higher glycolysis intermediate levels and correlation with CRC patient survival rates [60]. GLUT-1 expression in response to metformin was quantified using 3 different methods; immunoblotting, quantitative confocal imaging and fluorescent flowcytometry. Expression rates in HG were almost consistently stable across all verification methods and showing a slight, properly insignificant decline that could be

attributed to the abundance of glucose available to the cell in the absence of hypoxic conditions. As previously described, hypoxia drives the HiF1-mediated GLUT-1 overexpression in tumours. Other mechanisms are also known to regulate GLUTs expression, including hormonal factors such as estrogen, or transcriptional factors which are poorly understood in the case of GLUT-1 [60]. This study shows the occurrence of an HiF1-independent overexpression of glut-1 generally observed across LG cultures (Fig.12, 13, 16, 21), this becomes more significant after considering the GLUT-1 expression variance in response to metformin that was absent in HG. The overexpression of GLUT-1 detected in low glucose cultures outlines the aggressiveness of SW-948 cells, by portraying their effort to uptake more glucose. However, studies show that, while GLUT-1 overexpression affects glucose uptake, lipogeneses and tumour formation, it does not affect ATP levels [17] Indicating that this overexpression is not based solely on the cell's energetic needs.

The induction of a morphological switch towards the mesenchymal phenotype through high-glucose-induced-EMT is widely referred to in literature [61], and is known to correlate with an increased invasiveness and drug resistance [62]. Nonetheless, confocal imaging shows signs of EMT being present in LG cultures (Fig.15) which can be theoretically correlated with larger surface area for GLUT-1 to be detected in non-permeabilized SW-948 Cells. The addition of metformin, a suppressor/reverser of EMT transformation through AMPK actions [62] could therefore reduce the surface area available to detect glut-1 in non-permeabilized cells represented as a decline in 48hrs 3mM metformin treatments through confocal imaging and flowcytometry of gated single cell population (Fig.21 A). Another explanation arises when these results are compared to the dose dependent increased GLUT-1 expression patterns obtained from western blots, where not only surface GLUT-1 is measured, but also its inactive cytoplasmic levels, a proposed prostate cancer prognostic marker [19]. It could be argued that metformin hinders the localization of GLUT-1 to the cell surface where it is active. Nonetheless, metformin does seem to correlate with the upregulation of GLUT-1 mRNA levels and protein expression due to increased cellular stress (Fig 12, 16). A high throughput data analysis of flowcytometric events initially correlates with the confocal immunofluorescence quantification findings, but when gated to a much stricter refined population of similar granularity, GLUT-1 levels seem to increase in response to higher metformin concentrations (Fig 13, 21). In other words, metformin may be able to decrease GLUT-1 surface co-localization in the majority of treated cells, but a significant sub-population is still able to materialize its overexpression to an active form. The previous finding could be

attributed to an insufficient metformin treatment or a cellular resistance mechanisms which will be touched upon later. While the previous finding could offer another explanation for the conflicting results among test methods, it also stresses on the need to target the metabolic pathways rather than membrane receptors. GLUT-1 and other cell-surface proteins might prove useful as a prognostic tool, but as a therapeutic target, they would eventually suffer from drug resistance [18].

Estimation of OCT-1 mRNA levels, the main transporter of Metformin into the cells indicates a dose-dependent down regulation (Fig.19) regardless of glucose levels in the culture media. This hints at a drug repulsive mechanism adopted by the cells to decrease the intracellular accumulation of metformin. If GLUT-1 levels to be linked with metformin actions, a downregulated OCT-1 could provide an alternative rationale for the subsequent diminished expression levels of the former corresponding to higher metformin treatment (3mM). Regardless, OCT-1 regulation undoubtedly holds a pivotal role in defining the calibre of metformin effects, one that seems to be widely disregarded in many *in-vitro* studies by espousing the use of metformin levels that surpasses its possible accumulation in tissues, which could overcome the existence of low surface cationic transporter levels on used immortalized cell lines [14]. With that in mind, it would be unfitting to expect these high concentrations to attain similar reactivity *in vivo*. However, employing an alternative delivery method for metformin could be a feasible method to overcome this problem.

Mitochondrial content correlating to translocase of the outer mitochondrial membrane (TOMM) antibodies was also measured in various culturing and treatment situations to indicate the cell mitochondrial energetic dependency [63]. An increased content was observed when culturing in physiological glucose levels alone, in a hint towards the ability of these cells to engage higher OxPhos. However, the experiment Imply that the pinnacle of this increase sets at almost 1.5 times the content in high glucose when stressed by metformin regardless of the dose or exposure time. Increased mitochondrial content is also observed using HG but quickly falls down after 48 hours, which may indicate a reverted dependency to glycolysis. To inspect the functionality of this increased mitochondrial content, mRNA levels of the mitochondrial membrane bound UCP-2 was measured. A higher mitochondrial membrane potential is a driving factor for the production of ROS, which in turn stimulate the upregulation for UCP-2 expression in order to relieve the ROS stress to what seems to be an anti-oxidative stress defence mechanism [27]. With that in mind, an upregulated UCP-2 levels as observed in physiological glucose

treatments when compared to high glucose, is an indicator it-self for the highly glycolytic SW984 cell line's ability to reoperate their mitochondria to a certain capacity. The addition of the complex I inhibitor, metformin did indeed cause UCP-2 levels to be down regulated as it is thought to disturb the membrane potential. Interestingly, a complete pattern can be seen in cells cultured in high glucose, as metformin seems to increase UCP-2 levels in cells that are less likely to use the mitochondria to produce energy given the abundance of glucose. In the previous case, it can be thought that an increased uncoupling would result in an unregulated ETC flow, running endlessly without significant ATP production to initiate a negative feedback and therefore supporting TCA intermediate accumulation that might be needed to overcome the stress enforced by metformin. Howbeit, it is worth noting that mRNA levels of UCP-2 do not always reflect its protein expression as it seen in a variety of cell types that do not eventually express correspondence UCP-2 protein levels such in B-cells [27]. Therefore, a quantification of protein expression must be conducted on before drawing any solid conclusions. In Regard to TCA, PDK-2 mRNA levels were also measured. This enzyme is also known to be affected by ROS formation via its RORa-mediated inhibition of PDK-2 activity [36]. This inhibition could be the driving factor for the observed elevated mRNA levels of PDK-2 in untreated LG cultures (Fig.18). Similarly, the addition of metformin and its consequent restriction of ROS generation could offer an explanation for dose-dependent down regulation of PDK-2 as well as the possibility of it serving as a prognostic tool for metformin effectiveness on the mitochondria indicating a lower ROS formation. Taken together, metformin's actions on UCP-2 and PDK-2 in regard to the observable increased mitochondrial content in response to stress could establish its viability in inhibiting the mitochondria, which can prove to be more useful in the context of cancer treatment when the cell is more obligated to use it for energy production as observed in the parallel research on the more OxPhos-dependent SW1116 cell-line.

5.2 INCORPORATING METFORMIN IN CRC TREATMENT STRATEGY

The value of mitochondria in cell survival seems to exceed its energy bearing capabilities, the previous results suggest that this remains applicable to cancer cells exhibiting the Warburg metabolism, which are known to produce their needed ATP mainly from glycolysis [33]. It can be argued that the so called "dysfunctional" mitochondria in these cells, is able to perform an alternative role that maintains tumour growth through the previously mentioned uncoupled ETC activity and its subsequent flow of TCA

intermediates. Thus, an applied inhibition by drugs like metformin to the main unit of its OxPhos cycle, the electron transport chain may result in a subsequent reduction in these vital intermediates. Such inhibition has also been reported to initiate the imposingly evaded apoptotic process by cancer cells [29]. Pragmatically, it can be stated that adhering to this approach by using metformin single-handedly to eliminate cancer cells would not be sufficient, especially within the clinically tolerable concentrations. The prospect of diminishing ATP by an established ETC inhibitor such as Caulerpin has resulted in an AMPK-driven glycolysis to replenish the loss [4]. Therefore, a theoretical probability of adverse effects arising from an inadequate inhibition of ETC in some cancer phenotypes, promoting a glycolysis overdrive need to be taken into consideration. It is possible to speculate that the previous scenario may further induce invasiveness over growth inhibition in a non-zero sum game where the anti-tumour effects of metformin may end up as the weaker outcome. Hence, a thorough consideration of the initial tumour metabolic status would be recommended before deciding to use metformin. In addition to the cell's own metabolic profile, it has been suggested that the metabolic environment of the cell governed by its host tissue could influence metformin's capability [16], giving more significance to the association between tumor location and treatment success.

The most promising strategy of metformin use in cancers to date, and what can be recommended from the current work results compared to the study on SW1116 cell-line, is its utilization as an adjuvant agent after inducing a metabolic programming to OxPhos dependency (Fig.23), Positive outcomes were observed in various studies employing a cytotoxic agent such as 5-Fluorouracil (5-FU) to promote the needed energetic shift indicated by a longer cell cycle, and was able in combination with metformin to induce death in what referred to as "OxPhos addicted cells" [21]. Metformin also demonstrated a capability to reverse 5-FU-induced multidrug-resistant by countering EMT, even in small doses [62]. Moreover, its adjuvant benefits were inspected alongside radiation therapy [20] and is further established by analytical studies in CRC to be advantageous especially in its early stages [43]. However, given the complexity of metformin's modes of action, the physiological patient status is also thought to play a part in adjusting the weight of its molecular mechanisms. It is still unclear which of metformin's pathways is more prominent in assorted cancers [15], For example, the systematic pathway is predicted to play a heavier part in obesity and T2D patients [15, 62]. While detecting the expression of LKB1 and TSC2 by tumours, predicts a enhanced effectiveness of the cellular pathway (table 3) [15]. Thus, an informed decision of metformin use after regarding these aspects

would probably result in an improved treatment approach regarding doses, course duration and drug combinations.

TABLE 3 Predictors of Metformin Benefits in Cancers (originally published in the journal of molecular endocrinology 48 [15]

MARKER	SYSTEMATIC EFFECT	CELLULAR EFFECT
PATIENT INDICATORS (HOST)		
HIGH BMI	+	
PHYSICAL INACTIVITY	+	
HIGH FASTING INSULIN	+	
INSULIN RESISTANCE	+	
OCT EXPRESSION IN LIVER	+	
TUMOUR INDICATORS (RECEPTORS EXPRESSION/UPREGULATED PATHWAYS)		
IR/IGF1R EXPRESSION	+	
INCREASED PI3K/MTOR	+	
OCT EXPRESSION IN TUMOUR CELLS		+
LKB1 EXPRESSION		+
TSC2 EXPRESSION		+

The effect of long term use of metformin that has been linked to a reduced cancer incidents in diabetics [14, 42] may exceed its observable direct and indirect actions on tumour cells. The overall glycaemic control and cellular metabolism alterations resulting from metformin administration can be cautiously linked to the prevention of "onco" metabolites accumulation that are able to induce epigenetic changes compiling towards tumorigeneses. However, the previous claim needs to be investigated further.

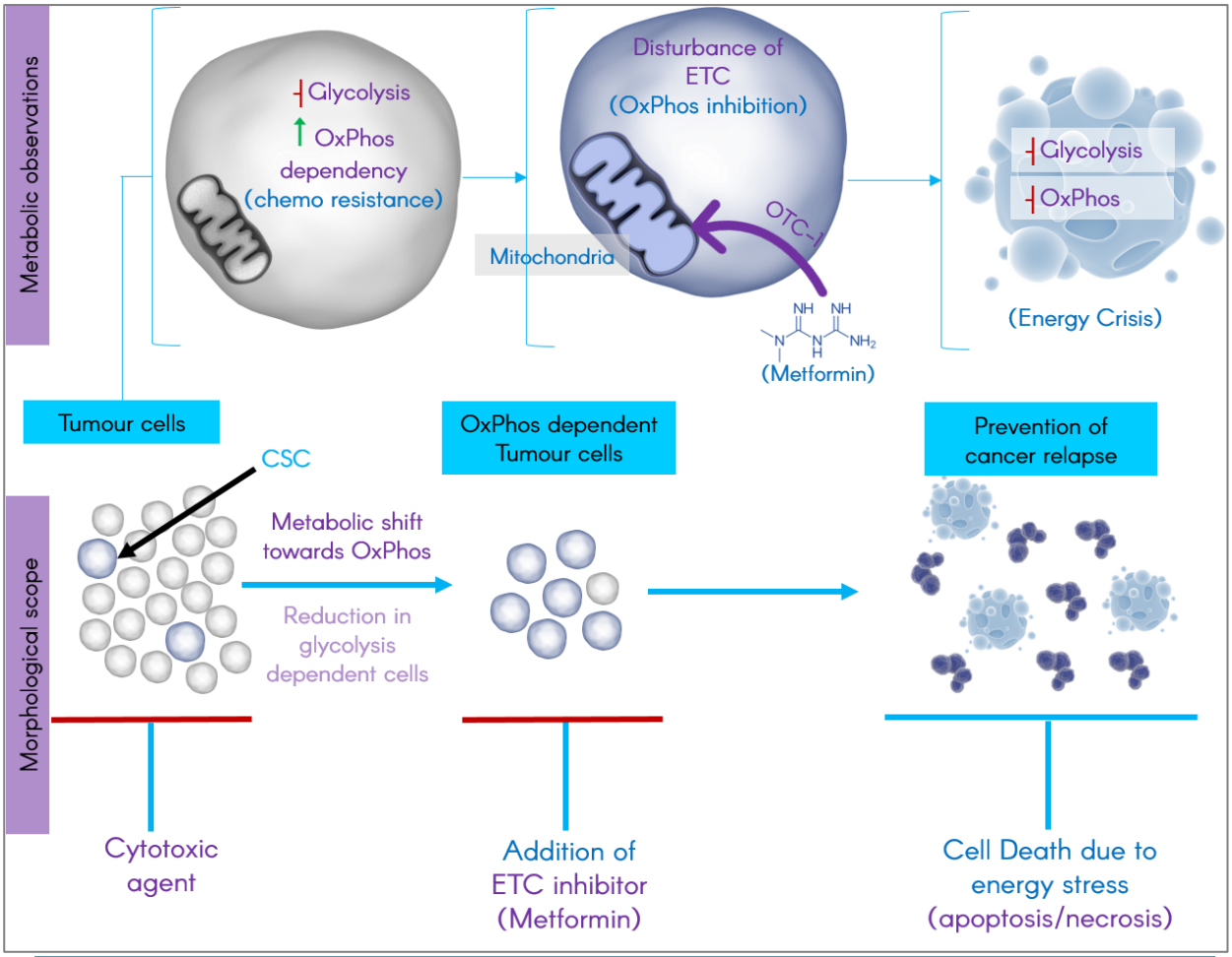

FIGURE 23 *Proposed metformin use in cancer treatment strategy*

Simplified treatment strategy incorporating the use of metformin to reduce chemo-resistance by targeting a metabolically reprogramed OxPhos-dependent cells and CSCs subpopulation responsible for cancer relapse. The delayed cellular effects of metformin in cancers suggests the need for alternative delivery mode for the effectiveness of this strategy.

CHAPTER 6. FUTURE RESEARCH PROSPECTS AND FINAL REMARKS

6.1 RESEARCH PROSPECTS

6.1.1 IMPROVMENTS ON THE CURRENT REASERCH

The current research inferences regarding metformin's effect on the mitochondria of glycolytic cancer cells can be further established by adapting some approaches that aim to enrich the *in vitro* work mentioned in Chapters 3 and 4. It would be interesting to study the role of hypoxia in correlation with GLUT-1 expression amid metformin treatment in both culturing conditions. As previously mentioned, HIF1 is an important upregulator of GLUT-1 expression in hypoxic conditions. Therefore, by analogously culturing the cells in a controlled air environment (or by adding cobalt chloride CoCl2) [60], it would be possible to assess whether the overexpression of GLUT-1 obtain a cumulative status induced by HiF-1, Metformin and lower glucose concentration collectively or it summits at certain expression level originating from a common promoting mechanism of the previously mentioned factors. This would be an important step towards determining the benefits of GLUT-1 prognostically. Secondly, it would be of a great value to test the advised energetic reprograming of the cells in both culturing conditions by combining metformin treatment with the administration of a cytotoxic agent of an established effectiveness in SW948 cell line such as VX-11e (targeting ERK2) 5-Fluorouracil or the antiandrogen, Bicalutamide [64]. The achievement of a metabolic shift can be first determined by measuring the extracellular flux, and if found a further investigation of stem cell markers in the treated population would indicate the potency of metformin towards CSC within clinical doses.

6.1.2 ENHANCING METFORMIN'S ACTIVITY

The substantial affinity of metformin towards the mitochondria has been mentioned in section 1.5.2, and was indicated in literature to attain a 1000-folds higher concentration in the mitochondrial matrix in comparison to the serum levels [46]. Be that as it may, the manifestation of its antidiabetic effects in the body was reported to have a delay of several days after treatment, and vary according to OCT-1 polymorphisms in different patients [38]. Moreover, the current results indicate the likeliness of cellular response

towards downregulating OCT-1 subsequential to metformin treatment. this adaptory reaction would result in reducing the uptake of metformin into the cancer cell, representing a critical obstacle in its anti-cancer application. On that account, producing an alternative strategy to deliver metformin into the cell could be ideal to exploit its anti-tumour effects within a therapeutic concentration, and potentially deviate from OTC-1 downregulation implications. There is indeed ongoing research towards manufacturing prodrugs to metformin that are more lipophilic [38]. Theoretically, this is possible to achieve chemically by adjusting its structurally available apolar hydrocarbon sidechain [14]. However, such methodology may result in increased drug toxicity. Regardless, exploring a physically-oriented approach could prove useful in the utilization of metformin in CRC treatment. For instance, metformin sustained release tablets are commonly avoided in diabetic use due to its consequential handicapped absorbance from the small intestine [38]. The pervious drug form might be useful to consider in CRC treatment as it would probably achieve higher concentrations and prolonged exposure of the metformin in the colon. A more universal approach, is to test whether metformin can be delivered to the cell with the help of a nanocarrier such as graphene. Taking advantage of graphene's micro sheets cellular penetrative potential [65] added to the conjugation of specific legends [66] towards CSC population would theoretically achieve an enhanced permeability of metformin to the cells of interest. Finally, the combination of metformin treatment with other well tolerated substances such as Vit-K (proposed UCP-2 inhibitor) could be an interesting prospect in cancer prevention or decreasing relapse occurrence in a non-cytotoxic manner.

6.2 CONCLUSIONS

Inclusive insights that may satisfy our need for understanding the originating factors of cancers and remove the ambiguity surrounding its methods of prevention and treatment approaches, maybe still far from reach. The units of our multicellular organisms have evolved to co-exist and cooperate from an undifferentiable solo living ancestor through endless regulating mechanisms. Proliferation being a vulnerable process, is closely monitored alongside its precursory signalling pathways through an array of checkpoints and opposing mechanisms, suggesting an everlasting risk of cancerous behaviour. To admit that what we consider as a disease and a burden for the community is possibly a primitive survival technique by the cell is a step towards innovative thinking towards a dynamic solution. The genetic code of our cells has undergone uncountable upgrades since its foundation in ancestor cells and appears to still contain within its nucleotide triplicates, exploitable mechanisms that is unfitting to the uniformity of a multicellular

organism. Nonetheless, these mechanisms could provide haven to a stressed cell. While this genetic material has evolved to be preserved from outside interference (mutagens), it appears to be that cellular metabolites are part of its adjusted cellular control through epigenetic changes that may, under the certain stress and environmental exposures, lead to complexed issues, one of them is cancer. The compelling magnitude of primary metabolic schemes in cancer development should assuredly give it more emphasis when discussing treatment options. Therefore, given the importance of the mitochondria in regulating these schemes further stated by cellular authorization to initiate apoptosis in case of malfunction, it is only sensible to investigate mitochondrial effectors to offer a promising direction in cancer management.

In conclusion, this dissertation demonstrates the ability of metformin within its therapeutic concentrations to affect the mitochondria of a glycolysis-dependant CRC cell line to some extent, manifested as a reduced cellular proliferation. However, and after comparing its actions in more OxPhos-dependent cells, following a metabolic programming strategy towards OxPhos would better utilize its use in preventing cancer relapse by affecting the responsible CSCs and CCCs population. The current work also provides an evident importance to the use of physiological glucose levels in culture media while assessing metformin actions in future research. The difference in results across used culture media proves that the use of high concentrations of glucose to culture cancer cell-lines would indeed provide accelerated proliferation, but it does not represent a fast-forward function that maintains the rates of underlaying molecular mechanisms in response to treatment, especially when testing a metabolic drug like metformin. The results also show that GLUT-1 levels may give insights about metformin actions in the cell, but it is still unestablished if it may be used as a prognostic tool of its effectiveness. These alongside other stated observations may serve as a base for further investigations in cancer metabolic alterations and the use of metformin in reversing chemoresistance.

REFERENCES

1. David AR, Zimmerman MR. Cancer: an old disease, a new disease or something in between? Nat Rev Cancer. 2010;10:728–33. doi:10.1038/nrc2914.
2. Seyfried TN. Cancer as a metabolic disease: On the origin, management, and prevention of cancer. Hoboken N.J.: Wiley; 2012.
3. Kuipers EJ, Grady WM, Lieberman D, Seufferlein T, Sung JJ, Boelens PG, et al. Colorectal cancer. Nat Rev Dis Primers. 2015;1:15065. doi:10.1038/nrdp.2015.65.
4. Yu H, Zhang H, Dong M, Wu Z, Shen Z, Xie Y, et al. Metabolic reprogramming and AMPKalpha1 pathway activation by caulerpin in colorectal cancer cells. Int J Oncol. 2017;50:161–72. doi:10.3892/ijo.2016.3794.
5. Haigis PKM. Molecular Pathogenesis of Colorectal Cancer. New York, NY: Springer New York Heidelberg Dordrecht London; 2013.
6. Arnold CN, Goel A, Blum HE, Boland CR. Molecular pathogenesis of colorectal cancer: implications for molecular diagnosis. Cancer. 2005;104:2035–47. doi:10.1002/cncr.21462.
7. Akkoca AN, Yanık S, Özdemir ZT, Cihan FG, Sayar S, Cincin TG, et al. TNM and Modified Dukes staging along with the demographic characteristics of patients with colorectal carcinoma. Int J Clin Exp Med. 2014;7:2828–35.
8. Ahmed D, Eide PW, Eilertsen IA, Danielsen SA, Eknaes M, Hektoen M, et al. Epigenetic and genetic features of 24 colon cancer cell lines. Oncogenesis. 2013;2:e71. doi:10.1038/oncsis.2013.35.
9. Hagland HR, Berg M, Jolma IW, Carlsen A, Soreide K. Molecular pathways and cellular metabolism in colorectal cancer. Dig Surg. 2013;30:12–25. doi:10.1159/000347166.
10. Hagland HR, Soreide K. Cellular metabolism in colorectal carcinogenesis: Influence of lifestyle, gut microbiome and metabolic pathways. Cancer Letters. 2015;356:273–80. doi:10.1016/j.canlet.2014.02.026.
11. Halama A, Guerrouahen BS, Pasquier J, Diboun I, Karoly ED, Suhre K, Rafii A. Metabolic signatures differentiate ovarian from colon cancer cell lines. J Transl Med. 2015;13:223. doi:10.1186/s12967-015-0576-z.
12. Xu W, Wang F, Yu Z, Xin F. Epigenetics and Cellular Metabolism. Genet Epigenet. 2016;8:43–51. doi:10.4137/GEG.S32160.
13. Wong CC, Qian Y, Yu J. Interplay between epigenetics and metabolism in oncogenesis: Mechanisms and therapeutic approaches. Oncogene. 2017;13:97. doi:10.1038/onc.2016.485.
14. Viollet B, Guigas B, Sanz Garcia N, Leclerc J, Foretz M, Andreelli F. Cellular and molecular mechanisms of metformin: an overview. Clin Sci (Lond). 2012;122:253–70. doi:10.1042/CS20110386.
15. Dowling RJO, Niraula S, Stambolic V, Goodwin PJ. Metformin in cancer: translational challenges. J Mol Endocrinol. 2012;48:R31–43. doi:10.1530/JME-12-0007.

16. Cantoria MJ, Patel H, Boros LG, Meuillet EJ. Metformin and Pancreatic Cancer Metabolism. In: McCall KD, editor. Pancreatic Cancer – Insights into Molecular Mechanisms and Novel Approaches to Early Detection and Treatment: InTech; 2014. doi:10.5772/57432.
17. Young CD, Lewis AS, Rudolph MC, Ruehle MD, Jackman MR, Yun UJ, et al. Modulation of glucose transporter 1 (GLUT1) expression levels alters mouse mammary tumor cell growth in vitro and in vivo. PLoS One. 2011;6:e23205. doi:10.1371/journal.pone.0023205.
18. Venturelli L, Nappini S, Bulfoni M, Gianfranceschi G, Dal Zilio S, Coceano G, et al. Glucose is a key driver for GLUT1-mediated nanoparticles internalization in breast cancer cells. Sci Rep. 2016;6:21629. doi:10.1038/srep21629.
19. Carvalho KC, Cunha IW, Rocha RM, Ayala FR, Cajaíba MM, Begnami MD, et al. GLUT1 expression in malignant tumors and its use as an immunodiagnostic marker. Clinics. 2011;66:965–72. doi:10.1590/S1807-59322011000600008.
20. Lu C-L, Qin L, Liu H-C, Candas D, Fan M, Li JJ. Tumor cells switch to mitochondrial oxidative phosphorylation under radiation via mTOR-mediated hexokinase II inhibition--a Warburg-reversing effect. PLoS One. 2015;10:e0121046. doi:10.1371/journal.pone.0121046.
21. Denise C, Paoli P, Calvani M, Taddei ML, Giannoni E, Kopetz S, et al. 5-fluorouracil resistant colon cancer cells are addicted to OXPHOS to survive and enhance stem-like traits. Oncotarget. 2015;6:41706–21. doi:10.18632/oncotarget.5991.
22. Faubert B, Vincent EE, Poffenberger MC, Jones RG. The AMP-activated protein kinase (AMPK) and cancer: Many faces of a metabolic regulator. Cancer Letters. 2015;356:165–70. doi:10.1016/j.canlet.2014.01.018.
23. Monteverde T, Muthalagu N, Port J, Murphy DJ. Evidence of cancer-promoting roles for AMPK and related kinases. FEBS J. 2015;282:4658–71. doi:10.1111/febs.13534.
24. Thorsten Cramer, Clemens A. Schmitt. Metabolism in Cancer. Switzerland: Springer International Publishing; 2016.
25. Keshav Singh LC. Mitochondria and Cancer. New York, NY: Springer New York; 2009.
26. Lodish H, Berk A, Zipursky SL, Matsudaira P, Baltimore D, Darnell J. Molecular Cell Biology 5th Edition: W. H. Freeman; August 1, 2003.
27. Krauss S, Zhang C-Y, Lowell BB. The mitochondrial uncoupling-protein homologues. Nat Rev Mol Cell Biol. 2005;6:248–61. doi:10.1038/nrm1592.
28. Donadelli M, Dando I, Dalla Pozza E, Palmieri M. Mitochondrial uncoupling protein 2 and pancreatic cancer: a new potential target therapy. World J Gastroenterol. 2015;21:3232–8. doi:10.3748/wjg.v21.i11.3232.
29. Yadav N, Kumar S, Marlowe T, Chaudhary AK, Kumar R, Wang J, et al. Oxidative phosphorylation-dependent regulation of cancer cell apoptosis in response to anticancer agents. Cell Death Dis. 2015;6:e1969. doi:10.1038/cddis.2015.305.
30. Pitt MA. Overexpression of uncoupling protein-2 in cancer: metabolic and heat changes, inhibition and effects on drug resistance. Inflammopharmacology. 2015;23:365–9. doi:10.1007/s10787-015-0250-3.

31. Yu G, Liu J, Xu K, Dong J. Uncoupling protein 2 mediates resistance to gemcitabine-induced apoptosis in hepatocellular carcinoma cell lines. Biosci Rep 2015. doi:10.1042/BSR20150116.
32. Weinberg RA. The biology of cancer. New York, N.Y.: Garland Science; 2014.
33. Fang S, Fang X. Advances in glucose metabolism research in colorectal cancer. Biomed Rep. 2016;5:289–95. doi:10.3892/br.2016.719.
34. Barron C, Tsiani E, Tsakiridis T. Expression of the glucose transporters GLUT1, GLUT3, GLUT4 and GLUT12 in human cancer cells. BMC Proceedings. 2012;6:P4. doi:10.1186/1753-6561-6-S3-P4.
35. Jeong JY, Jeoung NH, Park K-G, Lee I-K. Transcriptional regulation of pyruvate dehydrogenase kinase. Diabetes Metab J. 2012;36:328–35. doi:10.4093/dmj.2012.36.5.328.
36. Jeoung NH. Pyruvate Dehydrogenase Kinases: Therapeutic Targets for Diabetes and Cancers. Diabetes Metab J. 2015;39:188–97. doi:10.4093/dmj.2015.39.3.188.
37. Brandi G, Tavolari S, Rosa F de, Di Girolamo S, Agostini V, Barbera MA, et al. Antitumoral efficacy of the protease inhibitor gabexate mesilate in colon cancer cells harbouring KRAS, BRAF and PIK3CA mutations. PLoS One. 2012;7:e41347. doi:10.1371/journal.pone.0041347.
38. Graham GG, Punt J, Arora M, Day RO, Doogue MP, Duong JK, et al. Clinical pharmacokinetics of metformin. Clin Pharmacokinet. 2011;50:81–98. doi:10.2165/11534750-000000000-00000.
39. El-Mir MY, Nogueira V, Fontaine E, Averet N, Rigoulet M, Leverve X. Dimethylbiguanide inhibits cell respiration via an indirect effect targeted on the respiratory chain complex I. J Biol Chem. 2000;275:223–8.
40. Quinn BJ, Kitagawa H, Memmott RM, Gills JJ, Dennis PA. Repositioning metformin for cancer prevention and treatment. Trends Endocrinol Metab. 2013;24:469–80. doi:10.1016/j.tem.2013.05.004.
41. Evans JMM, Donnelly LA, Emslie-Smith AM, Alessi DR, Morris AD. Metformin and reduced risk of cancer in diabetic patients. BMJ. 2005;330:1304–5. doi:10.1136/bmj.38415.708634.F7.
42. Luengo A, Sullivan LB, Heiden MGV. Understanding the complex-I-ty of metformin action: limiting mitochondrial respiration to improve cancer therapy. BMC Biol. 2014;12:82. doi:10.1186/s12915-014-0082-4.
43. Coyle C, Cafferty FH, Vale C, Langley RE. Metformin as an adjuvant treatment for cancer: a systematic review and meta-analysis. Ann Oncol. 2016;27:2184–95. doi:10.1093/annonc/mdw410.
44. Sakar Y, Meddah B, Faouzi MA, Cherrah Y, Bado A, Ducroc R. Metformin-induced regulation of the intestinal D-glucose transporters. J Physiol Pharmacol. 2010;61:301–7.
45. Zhou G, Myers R, Li Y, Chen Y, Shen X, Fenyk-Melody J, et al. Role of AMP-activated protein kinase in mechanism of metformin action. J. Clin. Invest. 2001;108:1167–74. doi:10.1172/JCI200113505.

46. Bridges HR, Jones AJY, Pollak MN, Hirst J. Effects of metformin and other biguanides on oxidative phosphorylation in mitochondria. Biochem J. 2014;462:475–87. doi:10.1042/BJ20140620.
47. Yu X, Mao W, Zhai Y, Tong C, Liu M, Ma L, et al. Anti-tumor activity of metformin: From metabolic and epigenetic perspectives. Oncotarget 2017. doi:10.18632/oncotarget.13639.
48. Prives C, Manley JL. Why Is p53 Acetylated? Cell. 2001;107:815–8. doi:10.1016/S0092-8674(01)00619-5.
49. Leibovitz A, Stinson JC, McCombs WB3, McCoy CE, Mazur KC, Mabry ND. Classification of human colorectal adenocarcinoma cell lines. Cancer Res. 1976;36:4562–9.
50. Shiau C-K, Gu D-L, Chen C-F, Lin C-H, Jou Y-S. IGRhCellID: integrated genomic resources of human cell lines for identification. Nucleic Acids Res. 2011;39:D520–4. doi:10.1093/nar/gkq1075.
51. Jhawer M, Goel S, Wilson AJ, Montagna C, Ling Y-H, Byun D-S, et al. PIK3CA mutation/PTEN expression status predicts response of colon cancer cells to the epidermal growth factor receptor inhibitor cetuximab. Cancer Res. 2008;68:1953–61. doi:10.1158/0008-5472.CAN-07-5659.
52. Tym JE, Mitsopoulos C, Coker EA, Razaz P, Schierz AC, Antolin AA, Al-Lazikani B. canSAR: an updated cancer research and drug discovery knowledgebase. Nucleic Acids Res. 2016;44:D938–43. doi:10.1093/nar/gkv1030.
53. Smith PK, Krohn RI, Hermanson GT, Mallia AK, Gartner FH, Provenzano MD, et al. Measurement of protein using bicinchoninic acid. Analytical Biochemistry. 1985;150:76–85. doi:10.1016/0003-2697(85)90442-7.
54. Schindelin J, Arganda-Carreras I, Frise E, Kaynig V, Longair M, Pietzsch T, et al. Fiji: an open-source platform for biological-image analysis. Nat Methods. 2012;9:676–82. doi:10.1038/nmeth.2019.
55. QIAGEN Mini Handbook. Qiagen: RNeasy Plus Mini Handbook. 2014. https://www.qiagen.com/no/resources/resourcedetail?id=1b6ef882-da8c-4cd3-8665-d273aed02b38&lang=en&autoSuggest=true. Accessed 11 Apr 2017.
56. QIAGEN Reverse Transcription Handbook. (EN) - QuantiTect Reverse Transcription Handbook - QIAGEN. https://www.qiagen.com/no/resources/resourcedetail?id=f0de5533-3dd1-4835-8820-1f5c088dd800&lang=en. Accessed 11 Apr 2017.
57. Arqués O, Chicote I, Tenbaum S, Puig I, G. Palmer H. Standardized Relative Quantification of Immunofluorescence Tissue Staining. 2012.
58. MTS | Abcam. 27/05/2017. http://www.abcam.com/mts-cell-proliferation-assay-kit-colorimetric-ab197010.html. Accessed 29 May 2017.
59. Jeon S-M, Chandel NS, Hay N. AMPK regulates NADPH homeostasis to promote tumour cell survival during energy stress. Nature. 2012;485:661–5. doi:10.1038/nature11066.
60. Macheda ML, Rogers S, Best JD. Molecular and cellular regulation of glucose transporter (GLUT) proteins in cancer. J Cell Physiol. 2005;202:654–62. doi:10.1002/jcp.20166.

61. Duan W, Shen X, Lei J, Xu Q, Yu Y, Li R, et al. Hyperglycemia, a neglected factor during cancer progression. Biomed Res Int. 2014;2014:461917. doi:10.1155/2014/461917.
62. Qu C, Zhang W, Zheng G, Zhang Z, Yin J, He Z. Metformin reverses multidrug resistance and epithelial-mesenchymal transition (EMT) via activating AMP-activated protein kinase (AMPK) in human breast cancer cells. Mol Cell Biochem. 2014;386:63–71. doi:10.1007/s11010-013-1845-x.
63. Paepe B de. Mitochondrial Markers for Cancer: Relevance to Diagnosis, Therapy, and Prognosis and General Understanding of Malignant Disease Mechanisms. ISRN Pathology. 2012;2012:1–15. doi:10.5402/2012/217162.
64. Yang W, Soares J, Greninger P, Edelman EJ, Lightfoot H, Forbes S, et al. Genomics of Drug Sensitivity in Cancer (GDSC): a resource for therapeutic biomarker discovery in cancer cells. Nucleic Acids Res. 2013;41:D955–61. doi:10.1093/nar/gks1111.
65. Li Y, Yuan H, dem Bussche A von, Creighton M, Hurt RH, Kane AB, Gao H. Graphene microsheets enter cells through spontaneous membrane penetration at edge asperities and corner sites. Proceedings of the National Academy of Sciences. 2013;110:12295–300. doi:10.1073/pnas.1222276110.
66. Liu J, Cui L, Losic D. Graphene and graphene oxide as new nanocarriers for drug delivery applications. Acta Biomater. 2013;9:9243–57. doi:10.1016/j.actbio.2013.08.016.

APPENDIX

TABLE 4 Detailed information regarding used products and instruments

Indicator		Product	Company	Reference	Notes
3.1 (Culture)	1	SW948 cell-line	Sigma (ECACC)	Supplied from SUS Gastrointestinal translational research unit	
	2	T-75cm^2 canted neck culture flask with vented cap	Falcon	353136	Surface: TC-Treated
	3	Dulbecco's Modified Eagle's Medium-high glucose	Sigma	D5671-500ml	25mM of Glucose (2~5x Physiological)
	4	DMEM, low glucose, GlutaMAX™ Supplement	Gibco®	21885-025	5mM of Glucose (Physiological range)
3.2 (Growth)	5	6-well plates, flat bottom.	VWR®	734-2323	TC-treated
	6	Dulbecco's Phosphate Buffered Saline	BioWest	L0615	w/o Calcium w/o Magnesium
	7	Trypsin-EDTA 1X in solution	BioWest	L0930-100	w/o Calcium w/o Magnesium w/ Phenol Red
	8	K940 trypan blue solution 0.4%	AMRESCO	K940-100ML	
	9	Bürker Counting Chamber	Marienfeld-Superior	0640230	
3.3 (MTS)	10	96-well plates	VWR®	10062-900	Data acquisition was done using accent software v 2.6, Thermo lab systems
	11	Metformin hydrochloride	Sigma-Aldrich	PHR1084-500MG	
	12	MTS Cell Proliferation Assay Kit (Colorimetric)	Abcam	ab197010	
3.4 (Western Blots)	13	Compact Tabletop Refrigerated Centrifuge	Kubota	2800	
	14	Cell scrapers	VWR®	734-2602	
	15	RIPA buffer	Prepared (see supplementary table 4)		
	16	Halt Protease and Phosphatase Inhibitor Cocktail	ThermoScientific	78441	
	17	Pierce BCA Protein Assay Kit	ThermoScientific	23227	
	18	TGX Stain-free Gel Kit	BioRad	1610181	
		TEMED	BioRad	casnr 10-18-9	
	19	Prestained Protein Ladder	ThermoScientific	26619	In Running buffer (see supplementary table 5)
	20	MagicMark™ XP Western Protein Standard	Invitrogen™	LC5603	
	21	PowerPac™ Basic Power Supply	BioRad	1645050	
	22	Criterion™ Blotter	BioRad	1704070	in Blotting buffer (see supplementary table 5)
	23	Microbiology Skim Milk powder	Merk	1.15363.0500	
	24	Tween-20	Melford	P1362	
	25	Anti-Glucose Transporter GLUT1 antibody	Abcam	(EPR3915) ab115730	in washing buffer TBST (see supplementary table 5)
	26	Goat Anti-Rabbit IgG H&L (HRP)	Abcam	ab97051	
	27	Pierce ECL Western Blotting Substrate	ThermoScientific	32106	

	28	ChemiDoc™ Touch Imaging System	BioRad	1708370	
	29	Image Lab Software	BioRad	V6.0	
3.5 (Confocal imaging)	30	24-well plates	VWR®	10062-896	
	31	4% paraformaldehyde	Sigma-Aldrich	P6148-500G	Courtesy of NKB
	32	FCS / PBS containing 0.1% Tween-20 (PBST)	(see supplementary table 5)		
	33	Anti-Glucose Transporter GLUT1 antibody	Abcam	[EPR3915] ab195020	(Alexa Fluor® 647)
	34	Donkey Anti-Rabbit IgG H&L	Abcam	ab150075	(Alexa Fluor® 647)
	35	Bisbenzimide H 33342	Abcam	ab145597	(Hoechst 33342)
	36	Mowiol	Borrowed from NKB group at CORE		
	37	ImageJ software	National institute of health, USA	1.51k	Fiji disruption
3.6 (Qpcr)	38	RNeasy Plus Mini kit	Qiagen	74104	QIAshredder (205311)
	39	NanoDrop™ One/OneC Microvolume UV-Vis Spectrophotometer	Thermo Scientific™	ND-ONE-W	
	40	QuantiTect Reverse Transcription Kit	Qiagen	205311	
	41	Hs_SUCLA2_1_SG	Qiagen	QT00102788	
	42	Hs_UCP_1_SG QuantiTect Primer Assay	Qiagen	QT00014140	QuantiTect Primer Assay Product ID: 205311
	43	Hs_PDK2_1_SG QuantiTect Primer Assay	Qiagen	QT00038262	
	44	Hs_SLC2A1_1_SG QuantiTect Primer Assay	Qiagen	QT00068957	
	45	Hs_SLC16A3_1_SG QuantiTect Primer Assay	Qiagen	QT00085855	
	46	Hs_SLC22A1_1_SG QuantiTect Primer Assay	Qiagen	QT00019572	
	47	Hs_HSP90AB1_2_SG QuantiTect Primer Assay	Qiagen	QT01679790	
	48	Hs_RRN18S_1_SG QuantiTect Primer Assay	Qiagen	QT00199367	
	49	TE buffer	Borrowed from Eichacker, Lutz lab at CORE		
	50	SYBR Green PCR Kit	Qiagen	218073	
	51	Lightcycler 96	Roche	5815916001	
	52	Lightcycler software	Roche diagnostics international ltd	V 1.1.0.1320	
3.7 (Flow)	53	Anti-TOMM20 antibody - Mitochondrial Marker	Abcam	[EPR15581] ab205486	Alexa Fluor® 488
	54	Accuri C6 flow cytometer			
	55	FlowJo	© FlowJo, LLC	v0.2	
	-	Phosphate Buffered Saline	Sigma	P4417-50TAB	One tablet added to 200 mL distilled water
	-	Ascent software			

	–	Muktiskan ascent	Thermo scientific		
	–	96 -Well PCR-Plates	Brand (Roche combatable)	781365	DNA, DNAse and RNAse free +film
	–	TE Buffer	Borrowed from Eichacker, Lutz lab at CORE		
	–	Ammonium per sulfate	Sigma		
	–	Tris ultrapure	Saveen werner ab	T1000-1	
	–	Methanol	Emsure	1.06009.2500	
	–	NaCl	Sigma-aldrich	31434n-1kg-r	
	–	Tween 20	Melford	P1362	
	–	B-mercaptoethanol	Borrowed from NKB group at CORE		
	–	Glycine	Duchefa biochemie	G0809.1000	
	–	SDS (Sodium dodecyl sulfate)	Sigma	1001056325 l4390-25g	

SUPPLEMENTARY TABLE 5 Preparation of Reagents

Reagent		Ingredient	Volume (conc.)	Notes
3.4 (Western Blots)	RIPA Buffer	Trion X 100	2.5 mL (1%)	Lysis Buffer: Protease Inhibitor (100X) + 1µL per 100 µL of RIPA buffer.
		10% SDS	10% SDS (0.1)	
		Sodium Deoxycholate (NaDOC)	1.25 g (0.5%)	
		1M Tris pH7.4	12.5 mL (50 mM)	
		5M NaCl	7.5 mL (150mM)	
		Distilled Water	217.125 mL	
	Running Buffer 10 X	Tris	30.3 g	1X: 100 mL (10X) in 900mL distilled water
		Glycine	144 g	
		SDS	10 g	
		Distilled Water	1 Litre	
	Blotting Buffer 10 X	Trizma base	7.5 g	To a total of 2.5 L 1X : 200 mL of 10X in 1800 mL distilled water
		Glycine	36 g	
		Methanol	500 mL	

		Distilled Water	2 Litre	
	Washing Buffer	Tris	96.8 g	Washing Buffer (TBST) 1X 100 mL of 10X + 1mL of tween20 + 900mL distilled water (pH:7.6)
		NaCl	320 g	
3.5	PBST	PBS-T 2%	1 Part	
		FCS	2 Parts	
		dH2O	7 Parts	

SUPPLEMENTARY TO SECTION 3.4 (WESTERN BLOTS)

(3.4.1 ANNEX) BCA RESULTS AND STANDARD CURVES

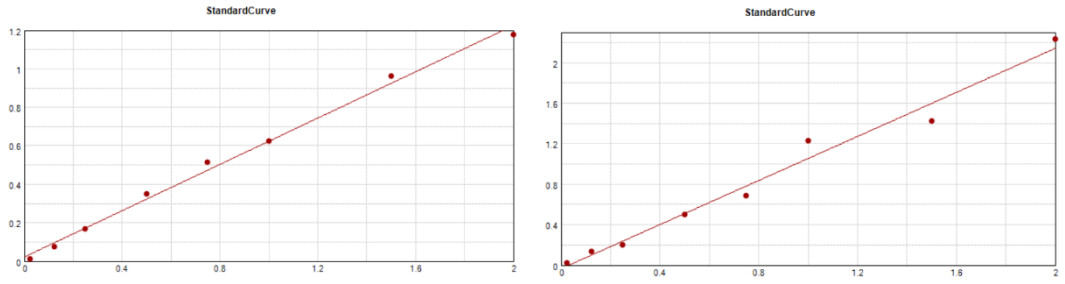

Lysate	1st Biological replicate	2nd biological replicate
	BCA RESULT	
I. HG control	1.849	0.762
II. HG 24 hrs 0.5 mM metformin	0.916	1.106
III. HG 24 hrs 3 mM metformin	0.609	0.711
IV. HG 48 hrs 0.5 mM metformin	1.029	0.66
V. HG 48 hrs 3 mM metformin	1.159	0.482
VI. LG control	1.175	0.377
VII. LG 24 hrs 0.5 mM metformin	0.661	0.339
VIII. LG 24 hrs 3 mM metformin	0.587	0.643
IX. LG 48 hrs 0.5 mM metformin	1.077	0.456
X. LG 48 hrs 3 mM metformin	0.901	0.356

(3.4.2 ANNEX) BAND ACQUISITION FROM LANE PROFILE

Acquired intestines for second membrane through lane profile in ImageLab

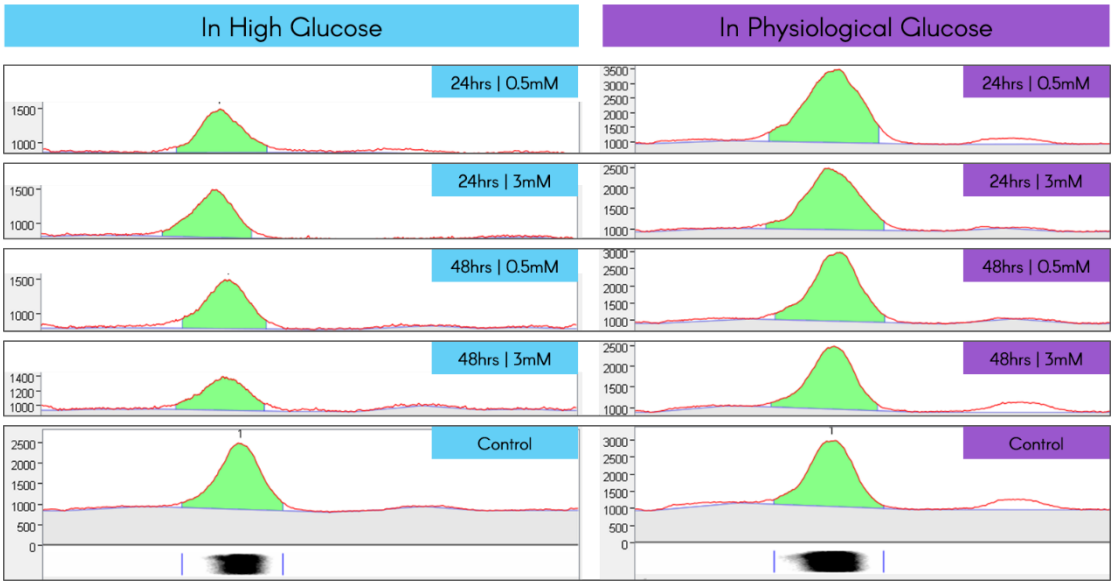

(3.4.2 ANNEX) STAIN FREE NORMALIZATION

Normalization Factors (NF) for second lysate (stain free gel)

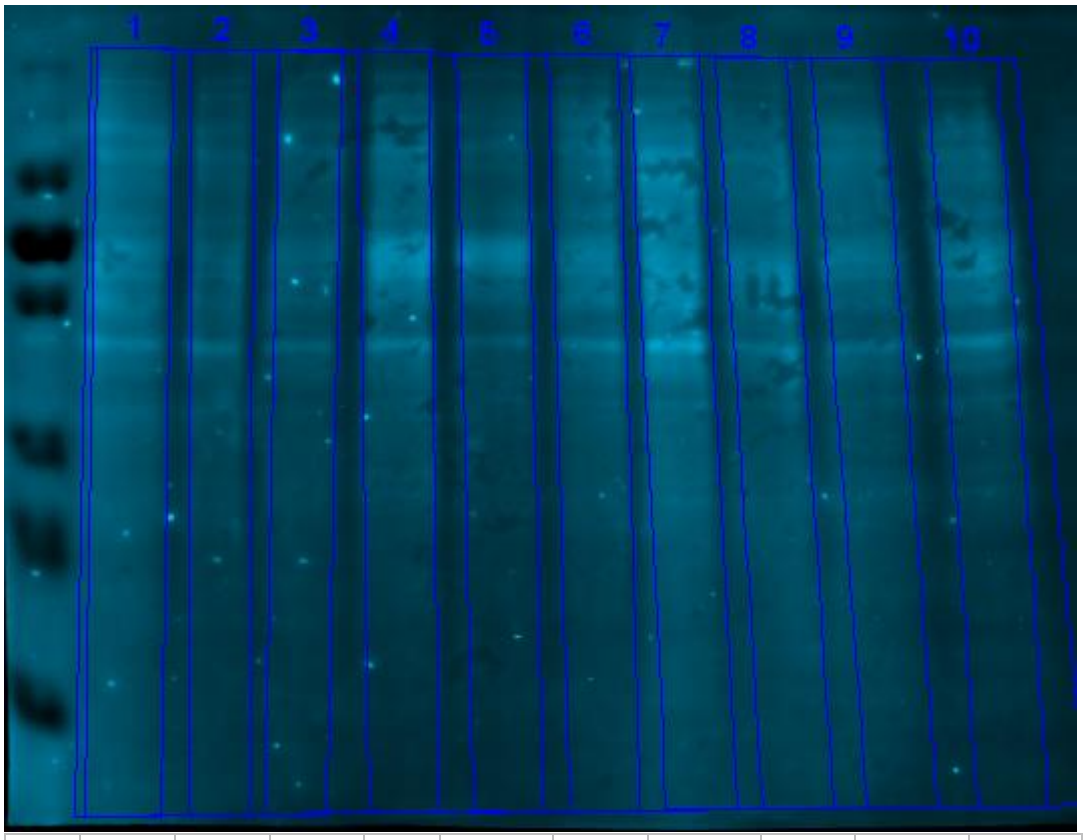

NF	1x	1.15x	1.36x	1.2x	1.26x	1.21x	2.43x	1.06x	1.45x	1.19x

SUPPLEMENTARY TO SECTION 3.6 (QPCR)

(3.6.1 ANNEX) RNA PURITY RESULTS

RNA sample	1st Biological replicate	2nd biological replicate
	(A260/280)	
I. HG control	2.06	2.03
II. HG 24 hrs 0.5 mM metformin	2.05	2.03
III. HG 24 hrs 3 mM metformin	2.02	2.02
IV. HG 48 hrs 0.5 mM metformin	2.06	2.02
V. HG 48 hrs 3 mM metformin	2.05	2.07
VI. LG control	2.04	2.02
VII. LG 24 hrs 0.5 mM metformin	2.05	2.02
VIII. LG 24 hrs 3 mM metformin	2.03	2.04
IX. LG 48 hrs 0.5 mM metformin	2.04	2.02
X. LG 48 hrs 3 mM metformin	2.03	2.05

(3.6.2 ANNEX) PRIMERS EFFICIENCY RESULTS

Tested primers Standard curves obtained by plotting Cq values against dilution Log quantity.

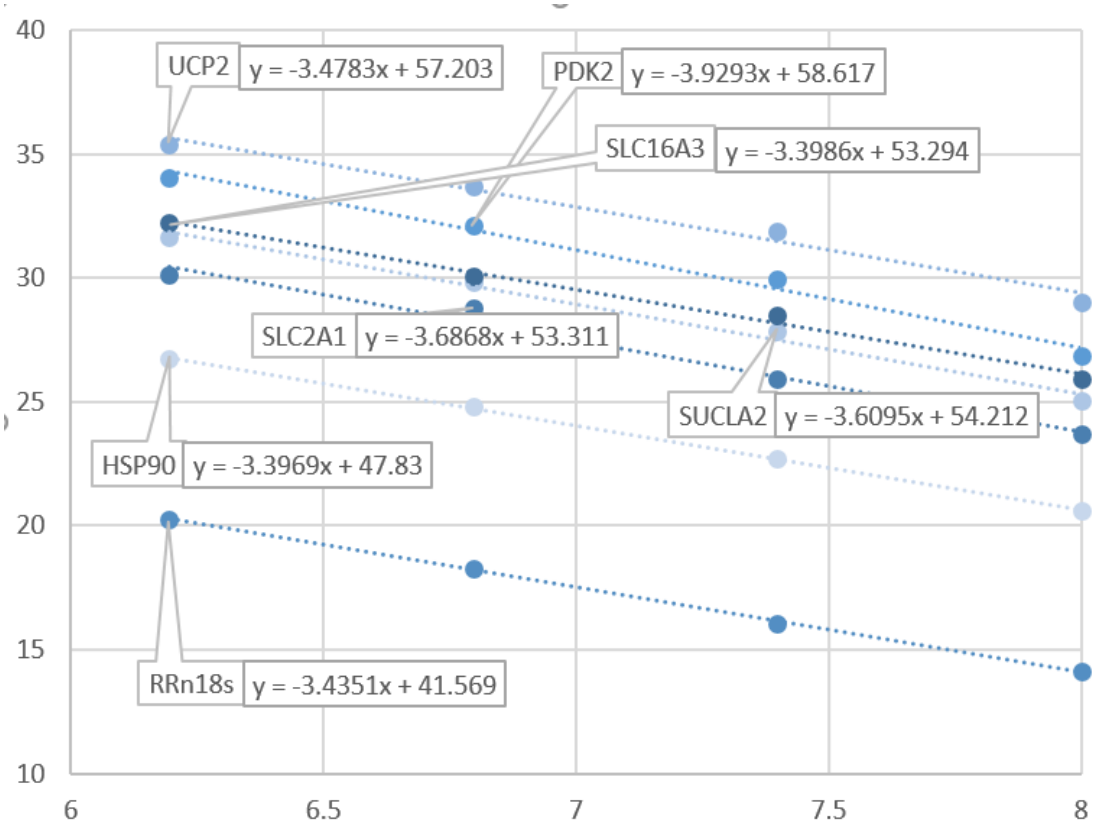

Primer	Slope	Efficiency	%
	EFFICIENCY = 10^(-1/SLOPE)		
HSP90	-3.396909729	1.969632559	97%
SUCLA2	-3.609540845	1.892533376	89%
UCP2	-3.478318207	1.938631481	94%
PDK2	-3.929301246	1.796793534	80%
RRn18s	-3.435112401	1.954840326	95%
SLC2A1	-3.686789916	1.867405664	87%